National Aeronautics and Space Administration

Young exoplanet discoveries from the K2 mission

Author: Trevor J. David (3262)
Eric E. Mamajek (3260), Gautam Vasisht (3262)

Introduction

Most known exoplanets orbit stars that are significantly older (>10^9 yr) than the timescales thought to be relevant in the formation and evolution of planets. This is a consequence of the facts that (1) there are few young stars near the Sun and (2) standard exoplanet surveys have deliberately avoided young stars due to the increased challenge of detecting planets amidst the variability characteristic of young stars. As a result, placing meaningful constraints on exoplanetary evolutionary timescales is difficult. Recently, the *Kepler* space telescope in its extended *K2* mission has observed thousands of young stars, leading to the discovery of the youngest known transiting exoplanets. A trend emerging from this initial population is that planetary radii appear to be larger at young ages. We report the detection of four new transiting exoplanets around young stars (Fig. 1 & 2), finding the youngest of these planets exhibits an anomalously large radius [1,2].

Methodology

We searched time series photometry from *K2* for transiting planets around stars with high-amplitude variability (an indicator of youth) and with galactic space motions consistent with membership to known young stellar populations. We acquired follow-up imaging and spectroscopy at W. M. Keck Observatory to prove the stars are single and that the transit signals must be due to planets rather than some other false positive scenario (e.g. an eclipsing binary star system).

We determined the ages of the planet-hosting stars via multiple methods. Stars lose spin angular momentum as they age due to gradual mass loss via magnetized stellar winds. A star's rotation period (determined from the brightness modulations seen in the *K2* data) is thus an indicator of stellar age. The strength of optical or ultraviolet emission lines originating from the stellar chromosphere can also be used to diagnose age. Finally, the star's temperature and luminosity (or, alternatively, density) can be compared with theoretical stellar evolution models for a coarse estimate of age.

Results

EPIC 247267267 b is a transiting sub-Neptune (R_P = 3.0±0.5 Earth radii) around a low-mass star believed to be a member of the Cas-Tau association. The proposed age (5—9 × 10^7 yr) would make it the second-youngest transiting exoplanet known to date. Theoretical predictions suggest the atmosphere of such a young planet may presently be losing mass through photodissociation via heating of the upper atmosphere by high-energy stellar radiation or internal heat generated by the planet's cooling core. Indeed, the planet's radius is anomalously large (Fig. 3) when compared to planets around mature, low-mass stars. This could be a sign that the planet's radius is still shrinking.

K2-233 is a nearby (distance = 69 pc) low-mass star with an age of 2.2—8.5 × 10^8 yr, corresponding approximately to the Epoch of Late Heavy Bombardment in our own Solar System. The star hosts three small transiting planets, with sizes relative to Earth of R_b = 1.40±0.06, R_c = 1.34±0.08, and R_d = 2.6 ± 0.1. The orbits, sizes, and separations of the planets all conform to patterns established from the population of mature exoplanets. Thus, there is no clear indication that the planets around K2-233 are different from those found around mature stars.

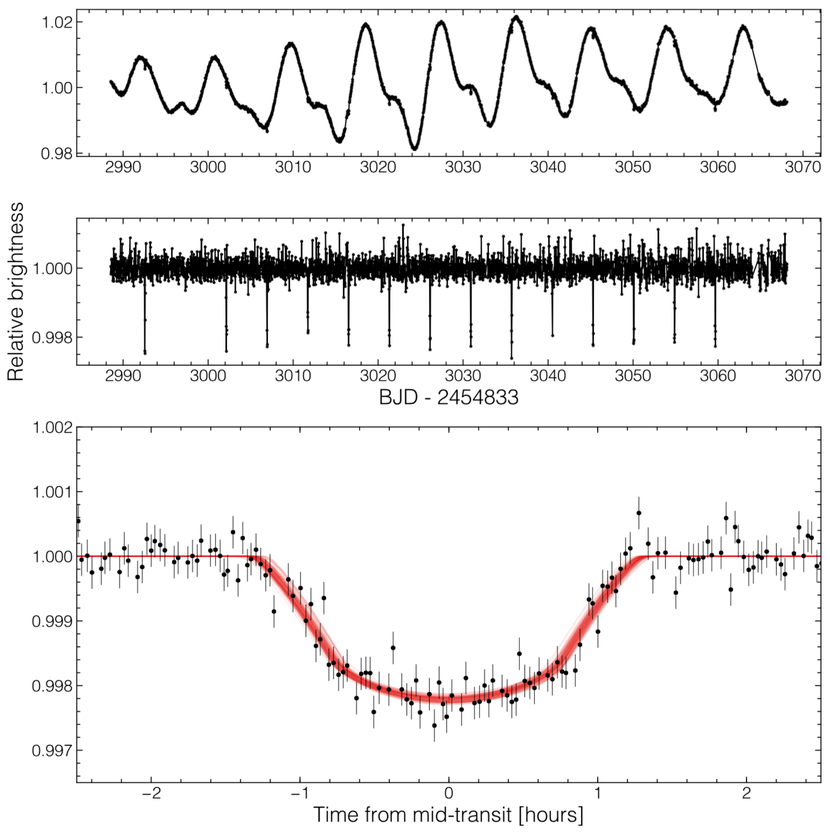

Figure 1. The *K2* light curve for EPIC 247267267 (top panel) with the stellar variability removed (middle) and phased to the planet's orbital period (bottom) with transit models shown by the red curves.

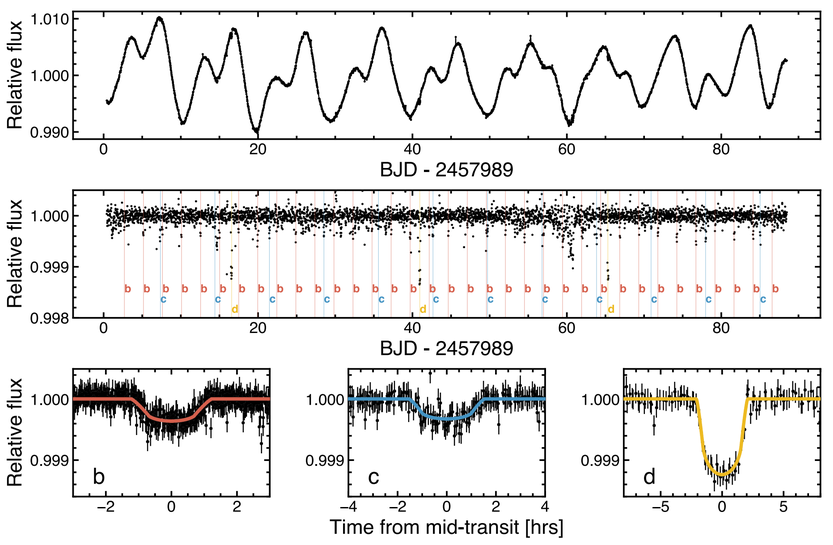

Figure 2. Same as above for K2-233 and its three planets (K2-233 b, K2-233 c, K2-233 d).

Conclusions

1. EPIC 247267267 b, an "adolescent" exoplanet with an age of <2% that of the Sun, is anomalously large when compared to similar planets around mature stars. One possible explanation is the planet's radius is still contracting due to atmospheric mass loss. This prediction can be tested with transit transmission spectroscopy: by observing the planet transit at many wavelengths simultaneously one might expect to see deep absorption in atomic hydrogen or helium lines which would indicate the presence of an extended cloud of escaping gas surrounding the planet.

2. K2-233 is a nearby young star hosting three transiting planets. Since the star is bright, it is an ideal target for follow-up studies to measure the planet masses and characterize their atmospheres. Our simulations show water vapor could be detected in the atmosphere of K2-233 d in a single visit with *JWST* (Figure 4).

3. A larger sample of young exoplanets is needed to determine whether the distribution of planet sizes is indeed dependent on age.

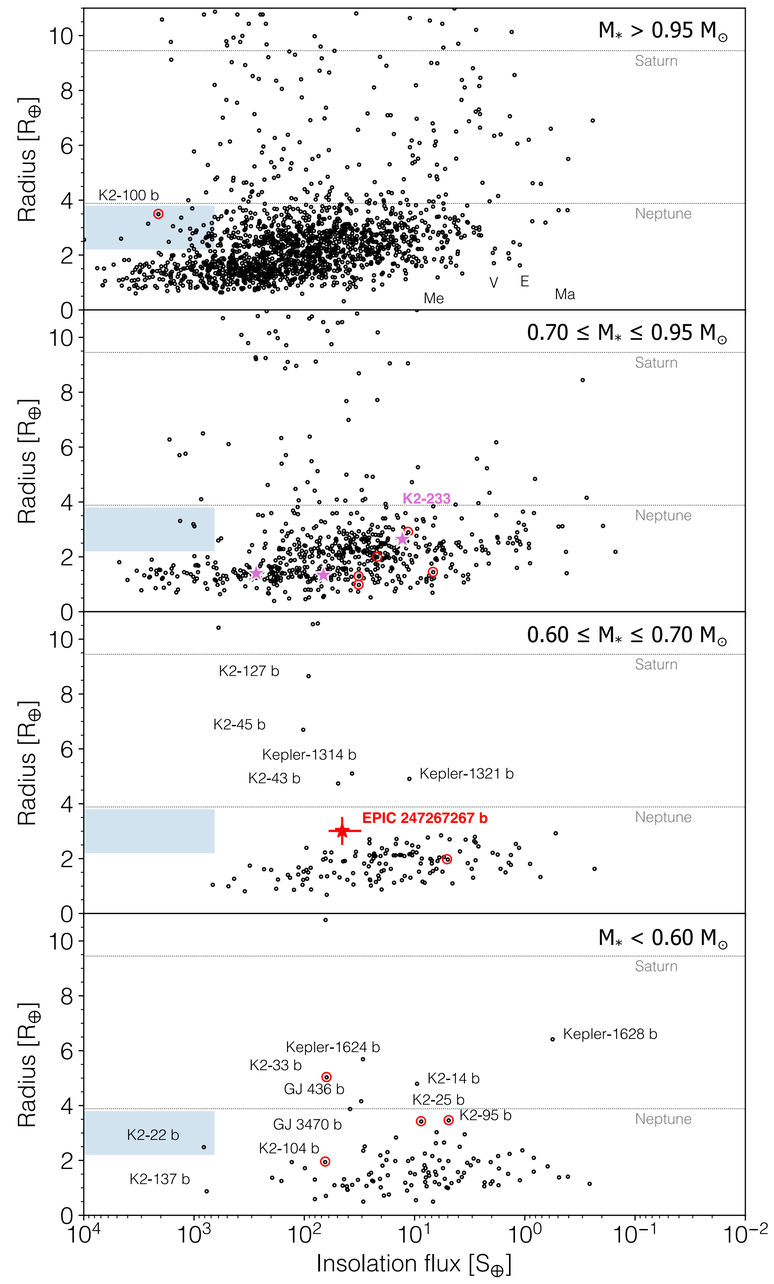

Figure 3. The distribution of transiting planets (black points) as a function of size and insolation flux (a proxy for orbital distance) for host stars in different mass ranges (indicated at upper right in each panel). Red circled points indicate known young planets. The purple and red stars indicate the K2-233 and EPIC 247267267 planetary systems, respectively. The positions of the inner Solar System planets are indicated in the top panel.

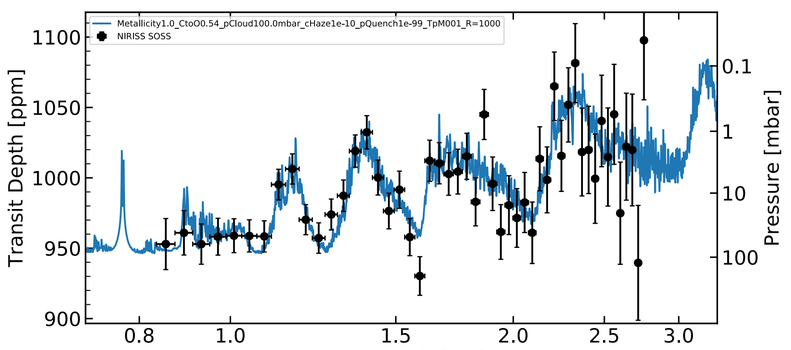

Figure 4. Simulated *JWST/NIRISS* transmission spectrum of the warm sub-Neptune K2-233 d. Variations in the transit depth as a function of wavelength, primarily due to absorption by water vapor in the atmosphere of the planet, should be readily detectable.

References

[1] David et al., "Three small planets transiting the bright young field star K2-233," *AJ*, 155, 222 (2018)

[2] David et al., "Discovery of a transiting adolescent sub-Neptune exoplanet in the Cas-Tau association with K2," in review at *AJ* (arXiv: 1801.07320)

National Aeronautics and Space Administration

Jet Propulsion Laboratory
California Institute of Technology
Pasadena, California

www.nasa.gov

Poster No. A-01

National Aeronautics and Space Administration

A Recipe to Bring Icy Bodies in the Habitable Zone

Interactions between Eccentric Planets and Debris Disks

Virginie FARAMAZ (Section 3262)

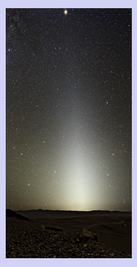

Exozodis are analogs to the Solar System Zodiacal cloud. They are made of hot dust that resides extremely close to a star. This dust is thought to originate from the evaporation and disruption of km-sized icy bodies, and tells us that the system contains a distant reservoir of km-sized bodies, and planet(s) that interact with it. It leads these bodies to permeate the most inner parts of the system, where they potentially bring water and organics on terrestrial-like planets in the Habitable Zone

OBSERVATIONAL CONSTRAINTS:

- Thanks to interferometric techniques that can probe a star's close environment, exozodis have been inferred around at least 11% of stars.
- These observations were puzzling because old stars (> 100 Myr) were found to host exozodis more frequently than young ones, where planets are thought to have long cleared their surroundings.
- In addition, many exozodis were detected in systems where no cold reservoir was detected.

WHAT MECHANISM CAN EXPLAIN THESE OBSERVATIONS ?

Mean-Motion Resonances

When two bodies are in *n:p* Mean-Motion Resonance (MMR), one body achieves *n* orbits when the other achieve *p* orbits.
Conjunctions always occur when bodies have the **same mutual positions** on their respective orbits. In the case shown here, bodies always achieve conjunction at the largest possible distance, which has a stabilizing effect. If they were to achieve conjunction at the smallest possible distance, they would become unstable at some point.

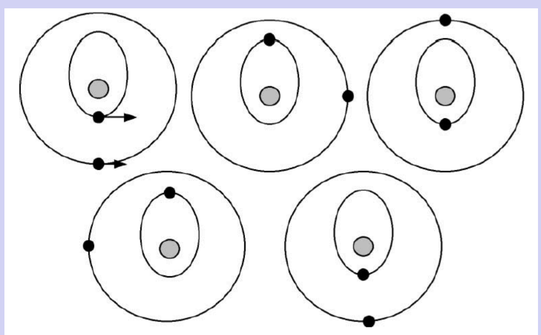

Two bodies in 2:1 MMR

From Laplace-Lagrange Theory, we know that if a small body is in MMR with an eccentric planet, it can experience very large modulations in eccentricity.
This wouldn't occur if the planet was on a circular orbit.

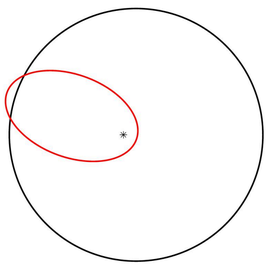

Example configuration that can be reached by a small body (red orbit) in 5:2 MMR with a slightly eccentric (e=0.1) planet (black orbit).

- If the scale of the system is small, small bodies in MMR can be directly set on a star-grazing orbits, evaporate or disrupt, and produce an exozodi. This is **direct production** of cometary orbits.
- If the scale of the system is large, the bodies do not approach the star close enough, but they can approach the chaotic zone, or even cross the orbit of the planet, where they can be scattered on star-grazing orbits. This is **indirect production** of cometary orbits.

INVESTIGATING MMR WITH AN ECCENTRIC PLANET

- Which resonances can achieve production of cometary orbits?
- Can this mechanism induce a flux of small bodies that is sufficient to produce the exozodis that are detected?
- In the case of direct production, cometary orbits will be produced very early. Can their production be maintained on large timescales?
- In the case of indirect production, small bodies will have to be scattered first, and therefore, cometary orbits will be produced with some delay. Can the delays be compatible with the late production (> 100 Myr) of exozodis?
- Can this mechanism produce an exozodi from an undetected cold reservoir?

Methodology and Walkthrough Example with the 5:2 MMR

Step 1: Use the Laplace-Lagrange Theory and phase-space diagrams to predict what eccentricity a given planet can induce on a small body in a given MMR.

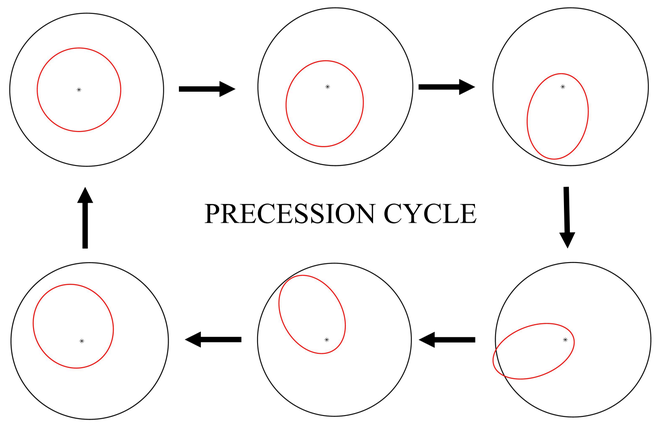

Small body (red orbit) and 0.1 eccentric planet (black orbit).

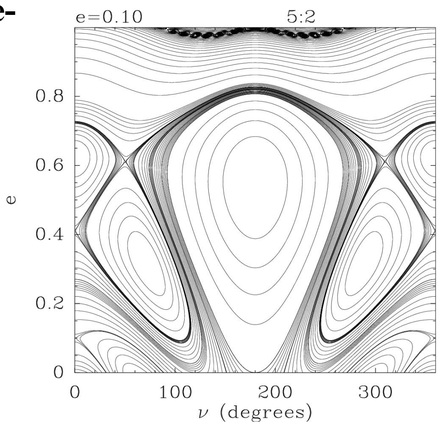

Example phase-space diagram. It tells us about the precession cycle and eccentricity modulations of a small body in 5:2 MMR with an 0.1 eccentric planet (displayed on the left).

The 5:2 MMR with an 0.1 eccentric planet can bring small icy bodies in the inner parts of a system. It does not depend on the planet's mass or semi-major axis.

Step 2: Study the timescales and rates thanks to N-body simulations.

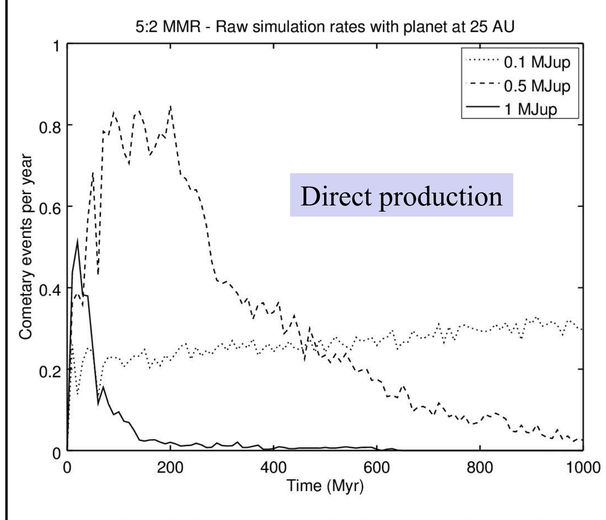

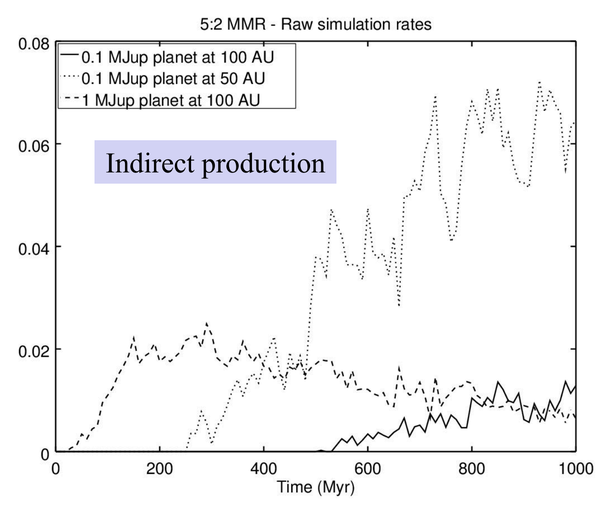

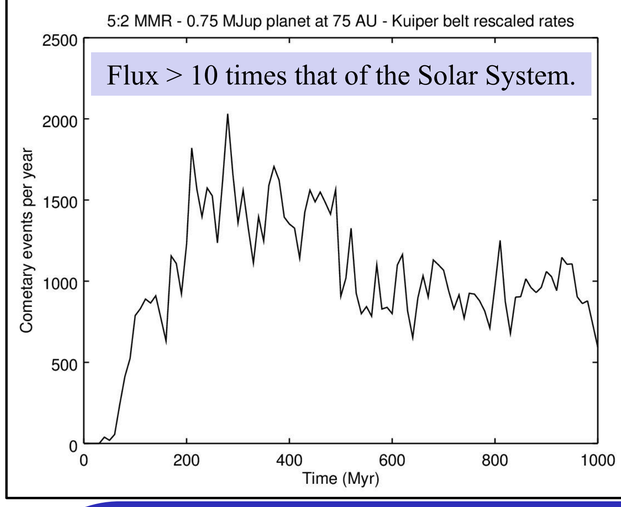

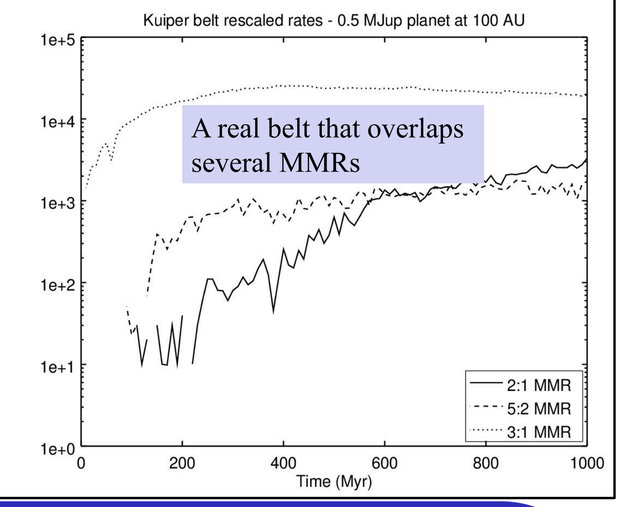

OVERALL CONCLUSIONS (Faramaz+ 2017)

MMRs WITH ECCENTRIC PLANETS

1) Can generate a **direct** flux of small bodies that can **be sustained over Gyr** timescales (planets with semimajor axis < 25 AU).
2) Can generate an **indirect** flux that can **start late** (after several 100 Myr) and **be sustained over Gyr** timescales (planets with semimajor axis > 25 AU).
3) Can produce a **detectable exozodi** from an **undetectable reservoir,** with mass similar to that of the Kuiper Belt.
4) Is a **robust** mechanism: it operate for **virtually any** planet semi-major axis on the typical scale of planetary systems, as well as for **several MMRs (**5:2, 3:1, 2:1).

IT HAS THE POTENTIAL TO EXPLAIN ALL THE OBSERVATIONAL CONSTRAINTS (FREQUENCY, HIGHER DETECTION RATE IN OLD SYSTEMS, ABSENCE OF CORRELATION WITH A COLD RESERVOIR)

Since typical exoplanetary systems contain both eccentric planets and reservoirs of icy bodies, could the input of water and organics on terrestrial-like planets in the Habitable Zone be as well typical? Ultimately, could life-bearing planets be typical?

National Aeronautics and Space Administration

Jet Propulsion Laboratory
California Institute of Technology
Pasadena, California

www.nasa.gov

Poster No. A-02

ExoPlanetary Systems in Polarized Light

Author: Maxwell A. Millar-Blanchaer (3262)

The GPIES Collaboration, Gautam Vasisht (3262), Eugene Serabyn (3262), Dimitri Mawet (Caltech), Ricky Nilsson (Caltech), Kaew Tinyanont (Caltech)

National Aeronautics and Space Administration

Debris Disk Morphology and Composition

Debris disks, extrasolar analogs to the Kuiper and Asteroid belts, can expose the grain growth histories of their systems through studies of their dust composition and can reveal the presence of unseen exoplanets through tell-tale morphological signatures. The GPIES Survey is searching for new debris disks in polarized using the Gemini Planet Imager's polarimetry mode.

Higher Contrasts in Polarized light

Observations of debris disks in scattered light are challenging due to the high contrast ratios between their emission and that of their host star. Polarimetry can reject unpolarized star-light, improving disk detection limits.

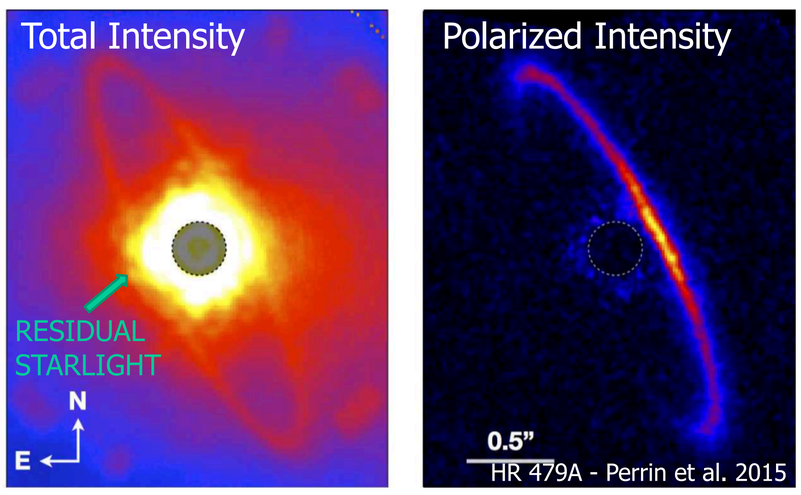

Morphological Signs of Unseen Planets

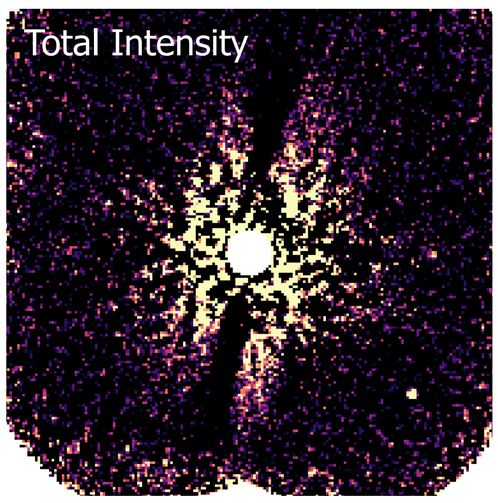

Total intensity dominated by residual starlight – No disk detection!

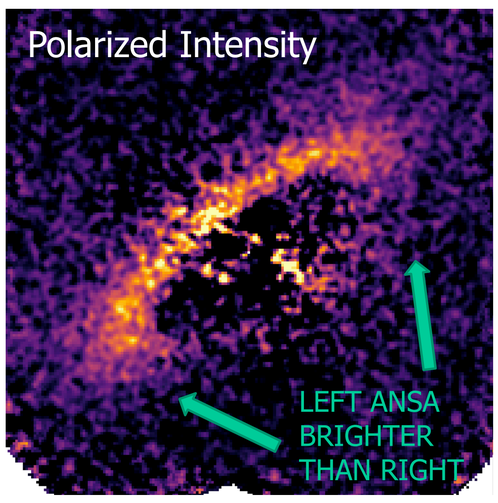

HD 157587 - Millar-Blanchaer et al. 2016

Strong disk detection. Brightness asymmetry likely caused by a planet-induced stellocentric offset.

Dust Scattering Phase Functions

Observations of the HR 4796A Debris Disk:

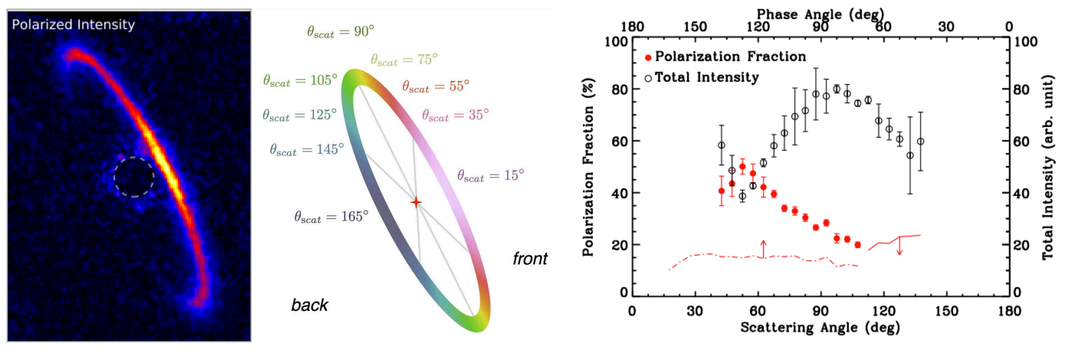

Astrophysical silicate dust models of varying size distributions:

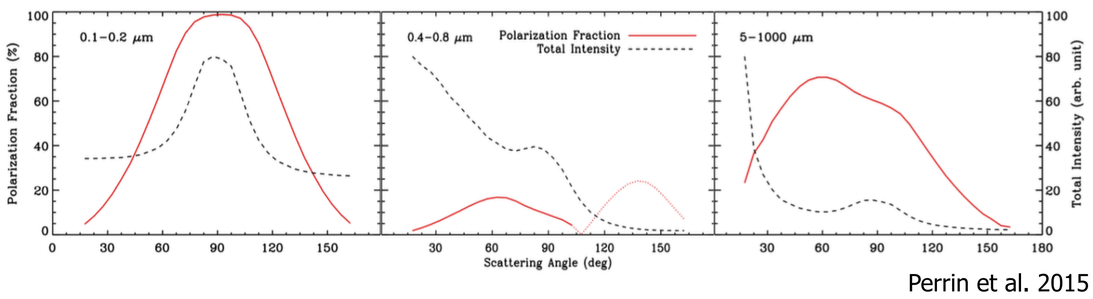

Perrin et al. 2015

Exoplanet and Brown Dwarf Atmospheres

Spectra of exoplanets and brown dwarfs have revealed signs of patchy clouds. However, very little is known about the true nature of these clouds, such as their height and their composition.

Polarized Atmospheres

Exoplanet and brown dwarf atmospheres can be polarized if there is an asymmetry in the atmosphere:

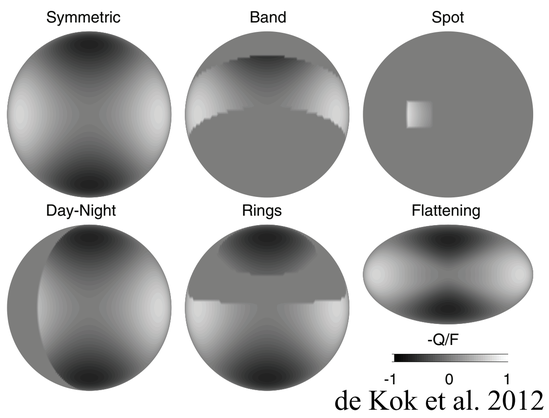

de Kok et al. 2012

Spectropolarimetry can provide a unique handle on cloud heights in these objects:

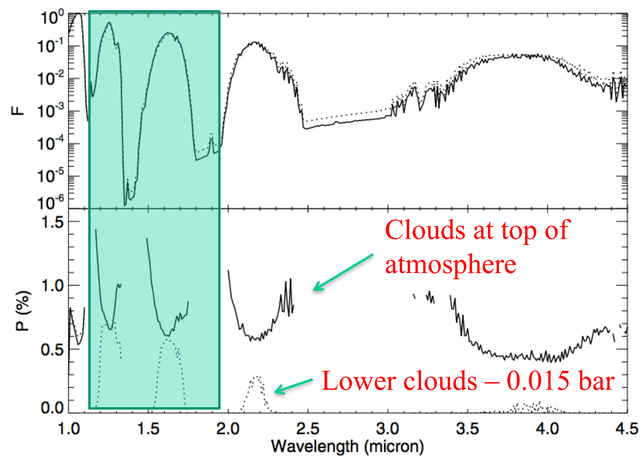

= WIRC+POL Wavelength Range

Spectropolarimetry with WIRC+POL

WIRC+POL is a new J- and H-band spectropolarimetry upgrade for the Palomar 200-inch telescope.

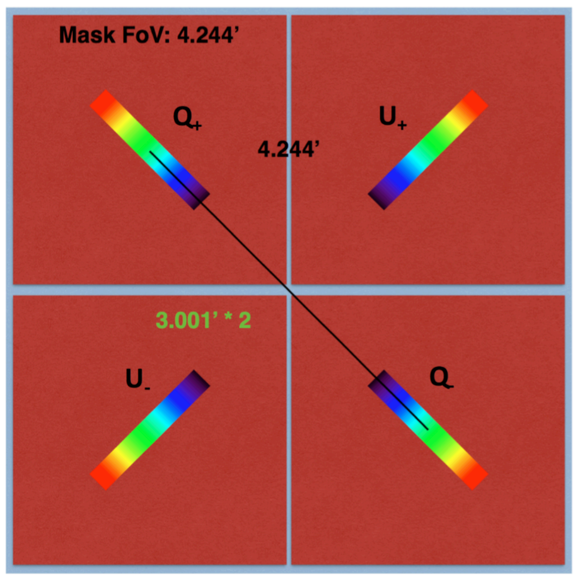

Cartoon image of the focal plane. A custom polarization grating creates four spectra, allowing us to measure Stokes Q and U in a single snapshot measurement.

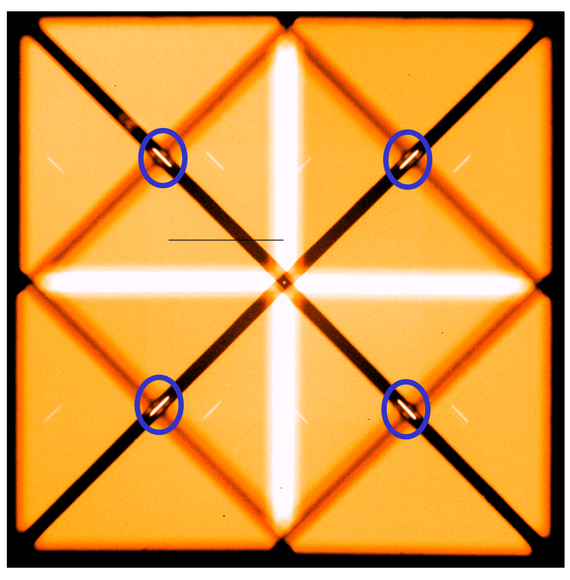

On-sky data: a focal plane mask creates a unique background image on the detector. The four spectra for the central source (blue circles) and two other sources are all visible.

The WIRC+POL Brown Dwarf Survey

A multi-year survey starting in the fall of 2017 to observe several 100s of brown dwarfs and systematically catalogue cloud properties across brown dwarf spectral types -> Implications for polarized exoplanets observations as well.

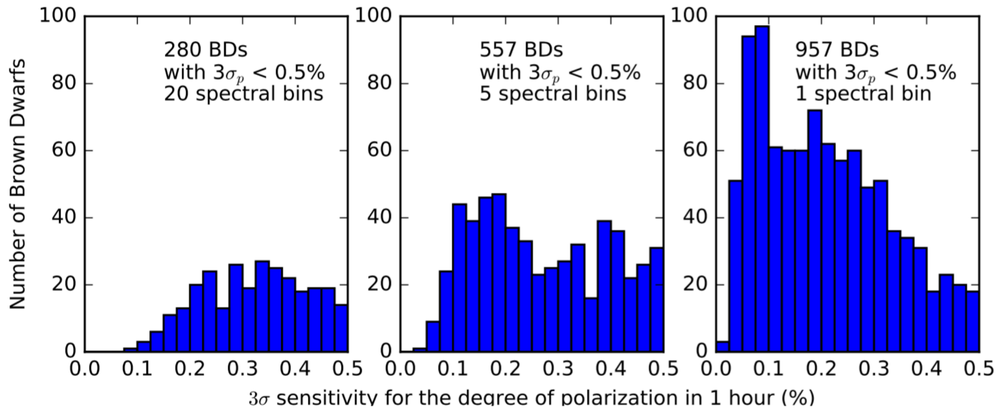

Simulated survey sensitivities for different spectral resolutions.

National Aeronautics and Space Administration

Jet Propulsion Laboratory
California Institute of Technology
Pasadena, California
www.nasa.gov

Poster No. A-03

National Aeronautics and Space Administration

Sodium pickup ions observed upstream of Mercury's magnetosphere

Jamie M. Jasinski[1] (3263)

Neil Murphy[1] (1210), Jim M. Raines[2], James A. Slavin[2], Leonardo H. Regoli[2], Daniel J. Gershman[3]

1. NASA Jet Propulsion Laboratory, Pasadena, CA; 2. University of Michigan, Ann Arbor, MI; 3. NASA Goddard Space Flight Center, Greenbelt, MA.

Introduction

- When a neutral atom is ionized in the heliosphere, it interacts with the magnetic (**B**) and electric (**E**) fields, and is "picked up" by (in this case) the solar wind plasma.

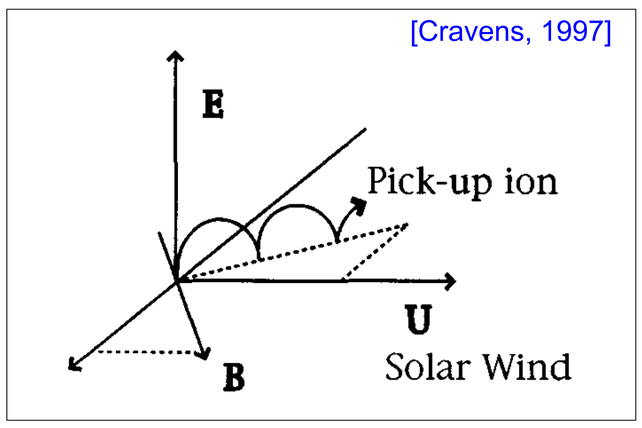

- The newly "picked up" ion is first accelerated along **E** and then gyrates around **B**. This results in a drift in the **E**x**B** direction.

- The resultant motion in space is a cycloid.

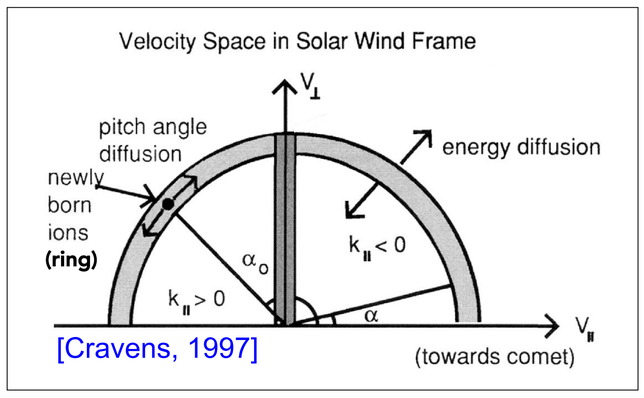

- In velocity space the cycloid translates to a **ring distribution**, which is scattered in pitch angle to a shell distribution.

- During our unique events, exospheric neutral sodium is ionised in the solar wind upstream of Mercury.

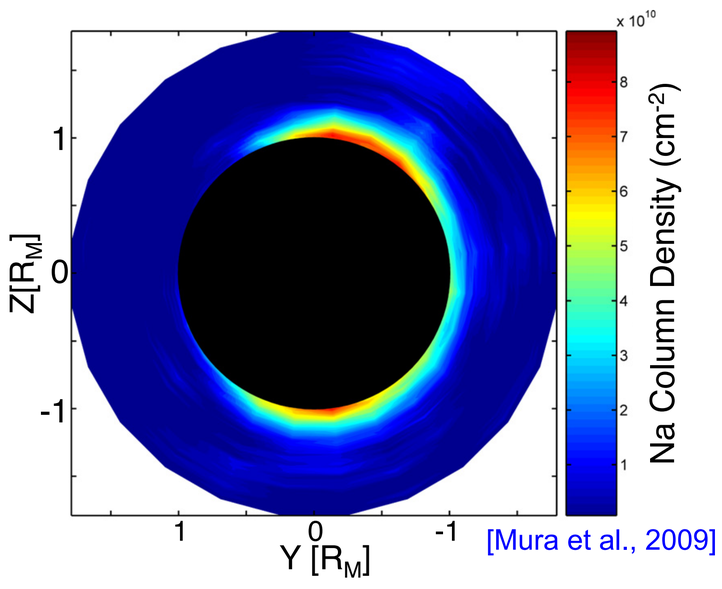

- Mercury's Na exosphere does not typically extend far from the planet and has a very small scale height.

- This is what makes these observations unusual, as neutral sodium is not expected to be observed so far from the planet. Either:
  - ✧ Something is causing a dramatic increase in the scale height
  - ✧ Or lower exospheric densities can be measured through pickup observations

Observations

- A typical MESSENGER spacecraft orbit through Mercury's magnetosphere. This orbit precesses in local time around the planet throughout the Mercury year.

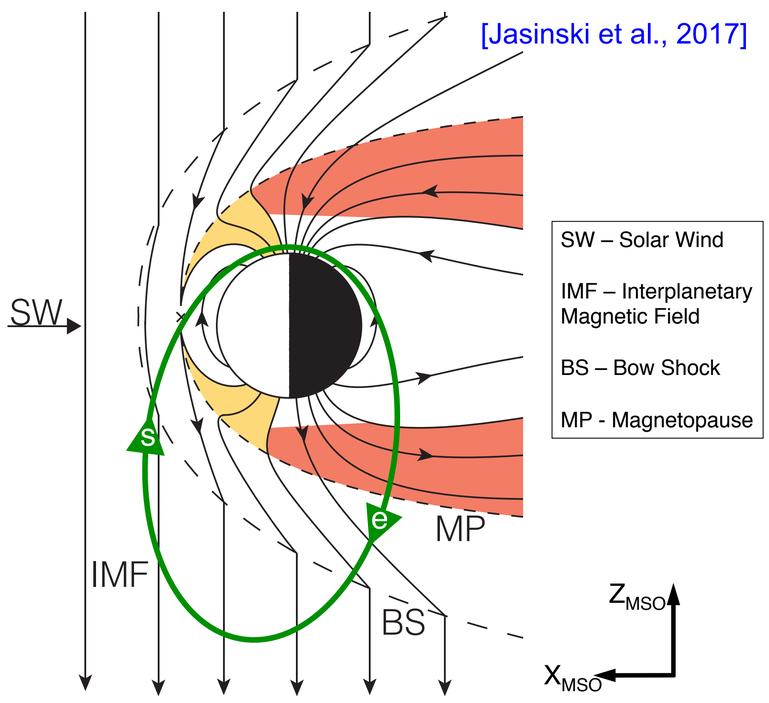

- Upstream of Mercury's bow shock we observe a sharp increase in Na^+ counts.

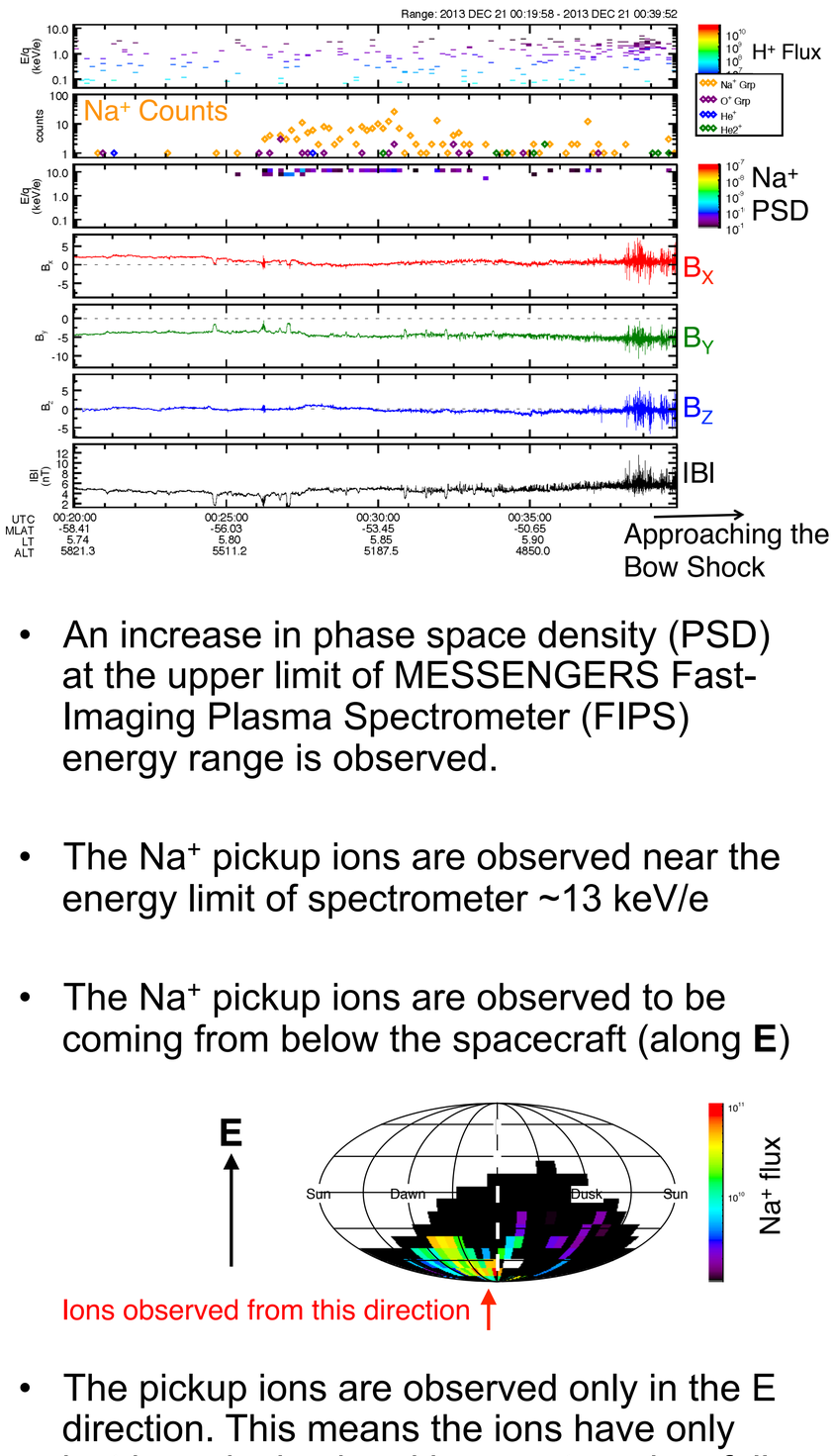

- An increase in phase space density (PSD) at the upper limit of MESSENGERS Fast-Imaging Plasma Spectrometer (FIPS) energy range is observed.

- The Na^+ pickup ions are observed near the energy limit of spectrometer ~13 keV/e

- The Na^+ pickup ions are observed to be coming from below the spacecraft (along **E**)

- The pickup ions are observed only in the E direction. This means the ions have only just been ionised and have not made a full gyration around the magnetic field.

- This shows that the ions are nongyrotropic.

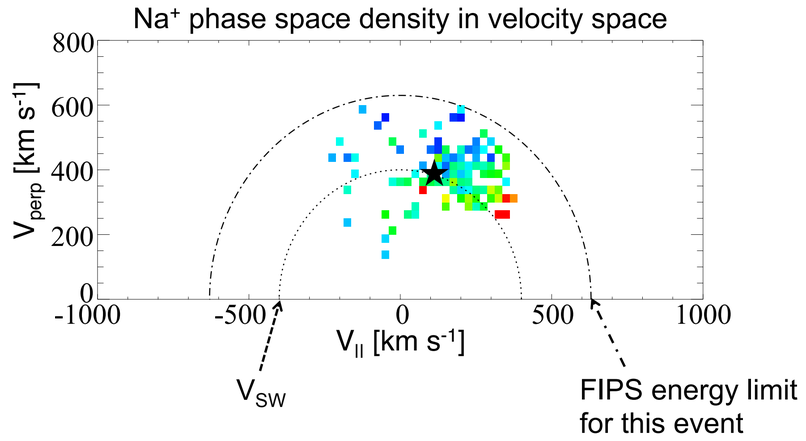

★ shows the model pickup ion ring distribution for the solar wind velocity using **V•B**/|B|

- The model ring distribution indicates the injection point of the pickup ions, which matches closely to the observations.

- Total of 23 sodium pickup ion events outside of Mercury's Bow Shock – shown below:
  - ≥ 5 counts/accumulation
  - ≤ 4 counts/accumulation

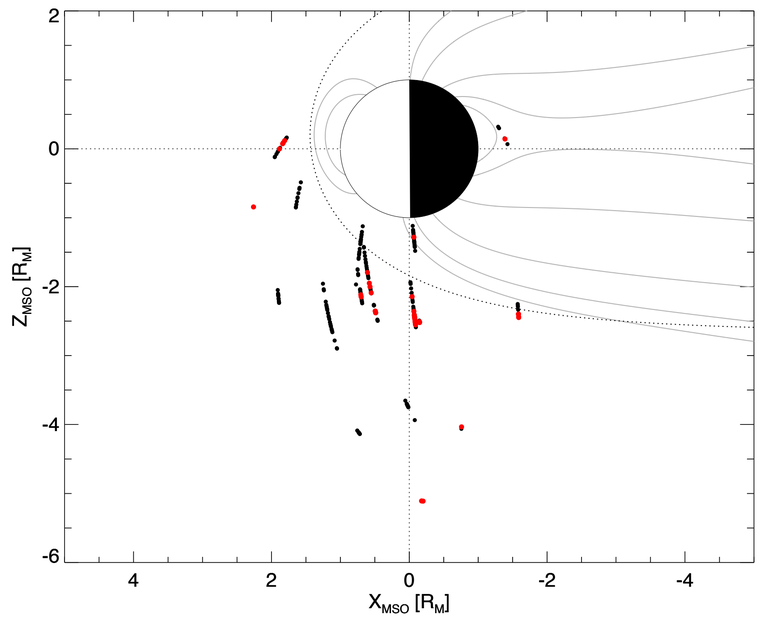

Discussion & Conclusions

1. Newly photoionized sodium, is observed upstream of the bow shock at much higher altitudes than the typical exosphere – transient phenomena caused by either intense meteroid volatilization or sputtering.

2. Due to direction of ion measurement and small interaction region (Na^+ r_g~ 4 R_M), the pickup ions are non-gyrotropic (similar interaction occurs at small comets: Glassmeier, 2017).

3. Currently calculating densities. Then we can infer neutral densities of the exosphere at this location during these events.

4. MESSENGER results are still revealing the nature of Mercury's interaction with the solar wind.

References: Cravens, 1997 (Cam. Uni. Press); Glassmeier, 2017 (Royal Soc. Press); Jasinski et al., 2013 (JGR); Jia et al., 2015 (JGR); Mura et al., 2009 (Icarus).

National Aeronautics and Space Administration
Jet Propulsion Laboratory
California Institute of Technology
Pasadena, California
www.nasa.gov

A-04

Chemical composition and physical properties of gases and volatiles in protostellar envelopes and Planet-forming disks: A new era of JWST

Author: Liton Majumdar[1]

Karen Willacy[1], William D. Langer[1], Paul F. Goldsmith[1] , Michael E. Ressler[1], Neal Turner[1], Geoffrey Bryden[1] , Thomas B. H. Kuiper[1] , & ngVLA Community Service (Round II) Team (other Co-Is from 3263 and 3266)

[1]Jet Propulsion Laboratory, California Institute of Technology, Pasadena, CA 91109, USA

I. Context

❑ **Observations of CO_2 in exoplanet atmospheres is one of the major science themes for JWST**. But CO_2 cannot be observed in the gas phase through rotational transitions in the far-infrared or sub-millimeter range due to its lack of permanent dipole moment. It has to be observed through its vibrational transitions at near- and mid-infrared wavelengths.

❑ **The protonated form of CO_2, $HOCO^+$, is an interesting alternative to track the gas phase CO_2 in the millimeter/sub-millimeter regime.**

Here, we report the detection of rotational emission lines of $HOCO^+$ in a Solar-type binary protostar IRAS 16293-2422 and discuss its implications for planet formation.

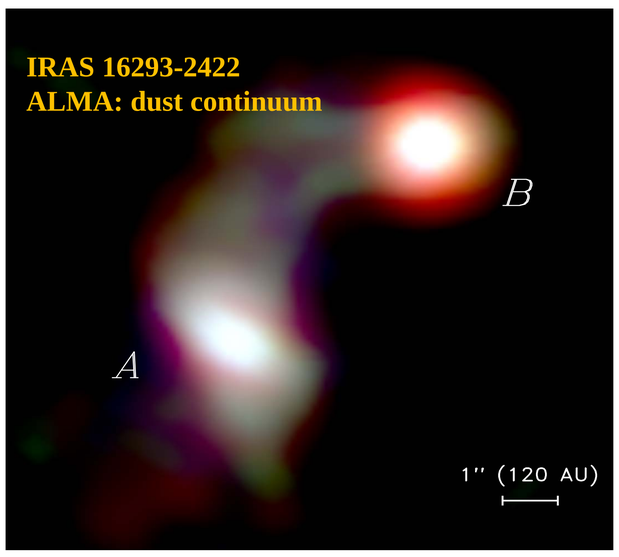

Three-color image above showing the continuum at 3.0 mm, 1.3 mm and 0.87 mm (ALMA Bands 3, 6 and 7) in red, green and blue, respectively.

II. Recent results:

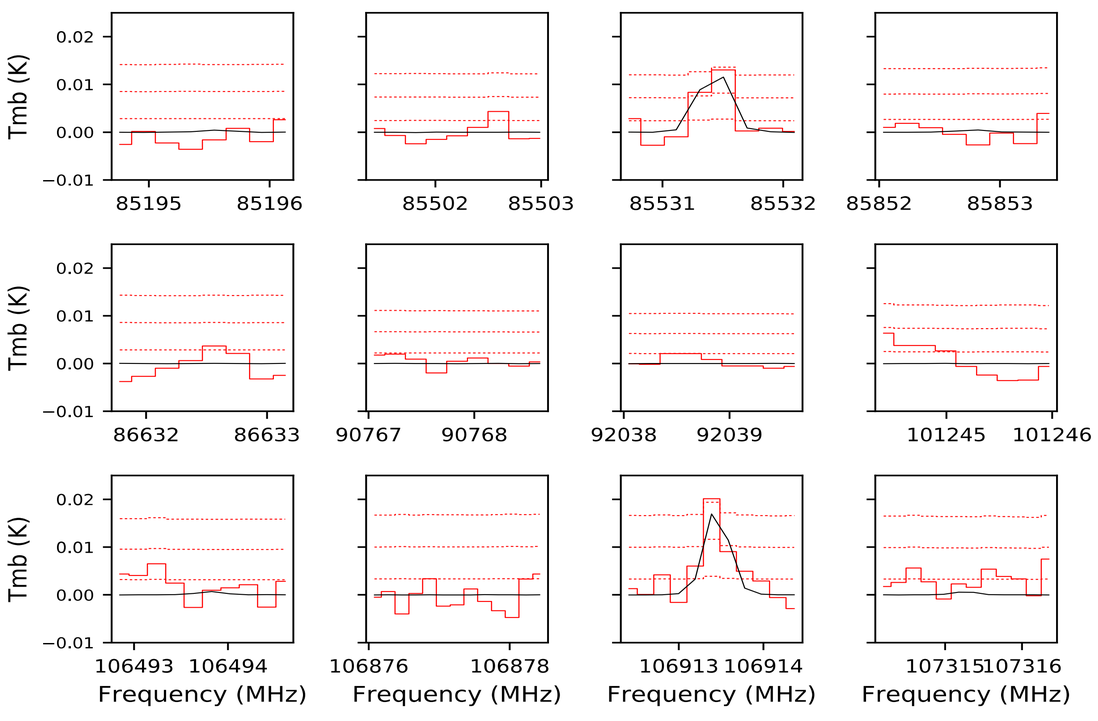

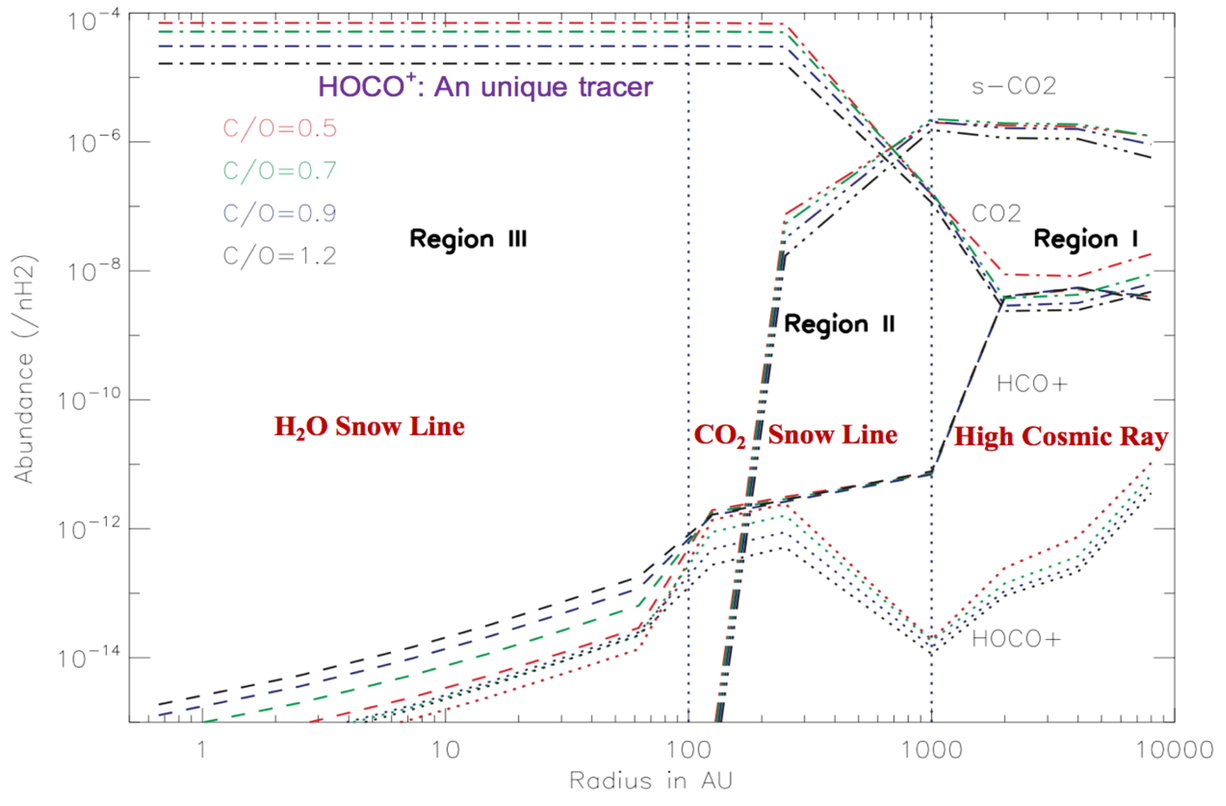

❑ **(Left Figure)** The red lines show the observed lines attributed to $HOCO^+$ in a solar type protostar IRAS 16293-2422 from **Majumdar et al. (2018)** using IRAM 30m Telescope. The black lines show the distribution of modelled spectra using MCMC simulation **(Majumdar et al. 2016, 2017, and 2018).** The thick line denotes the median of the distribution. The dark and light grey regions show the 68% and 95% confidence intervals. The dotted lines are 1**σ**, 3**σ** and 5**σ** noise levels. 1**σ** level is 2.7 mK.

❑ **(Right Figure)** Abundance with respect to H_2 for $HOCO^+$, HCO^+, and CO_2 predicted by our low-mass protostellar chemical-dynamical model for IRAS 16293-2422 as a function of distance to the central star. CO_2 designates the gas phase and s-CO_2 represents the CO_2 on the surface of grains. $HOCO^+$ is a tracer for three different regions in the protostellar envelope: 10000-1000 AU- **(high cosmic ray ionization regime)**; 800-200 AU- CO_2 desorption **(probe of CO_2 snow line)**; 150-10 AU- high temperature water chemistry **(probe of H_2O snowline).**

III. Summary & Conclusions:

❑ The detection of $HOCO^+$ in a protostar motivates a search in a protoplanetary disk, which would be a great achievement and would pave the way for better understanding of the overall **disk temperature structure**, **ionization structure, H_2O and CO_2 snow lines, overall C/O ratio** and link them with future observations of **CO_2 atmospheres in exoplanets**.

❑ The ngVLA (1.2-116 GHz) can provide a unique opportunity to detect the four strongest transitions of $HOCO^+$ at 21.38 GHz (1-0), 42.76 GHz (2-1), 85.53 GHz (4-3) and 106.91 GHz (5-4) in protoplanetary disks. **This effort is part of our ngVLA second round community service program.**

IV. Future direction:

❑ **Snowlines are key ingredients for planet formation. Providing observational constraints on the locations of the major snowlines is therefore crucial for fully connecting planet compositions to their formation mechanism.** Unfortunately, the most important snowline, that of water, is very difficult to observe directly in protoplanetary disks due to its close proximity to the central star. $HOCO^+$ can be used as an alternative to image the H_2O (and CO_2) snowline in Planet-forming region of disks using ALMA and ngVLA in the future**.**

❑ **Icy grain mantles are the main reservoir for volatile elements in star-forming regions across the Universe, as well as the formation site of pre-biotic complex organic molecules seen in our Solar System.** Motivated from $HOCO^+$ detection, as a part of our **JWST-MIRI GTO Program 1236 (PI: M. E. Ressler),** we will map the distribution of CO_2 and H_2O ices in several protostellar binaries in Perseus to identify when, and at what visual extinction, the formation of CO_2, and H_2O ice begins. Such high-resolution spectra together with gas phase observations will allow us to locate accurately their snowlines, as well as distinguish between different ice morphologies, thermal histories, and mixing environments as well.

V. Benefit to JPL:

❑ Chemical-dynamical model presented here will be used in the future together with 2D non-LTE radiative transfer model **(also in 3D , Majumdar et al. in prep)** to convert observed infrared molecular line fluxes, profiles and images from **JWST GTO Program 1236** from JPL to gas temperatures, densities and molecular abundances.

❑ Our model (together with our latest observations from NRO 45m and ARO12m Telescope) will also benefit spectroscopic predictions for future mission concepts **Origins Space Telescope (OST)** (where JPL is a part of Science and Technology Definition Team) and **Habitable Exoplanet Imaging Mission** (HabEx) (managed by JPL).

By providing predictions for OST and HabEx, JPL can make a vital contribution to the 2020 Decadal Survey and implementation of such potential missions.

Poster No. A-05

National Aeronautics and Space Administration

Mock galaxy catalogs for future weak lensing missions

Author: Albert Izard (3266)
Co-Authors: Alina Kiessling (3266), Eric Huff (3268)

We developed a fast method to generate hundreds of simulated surveys. We use the simulations to model observational systematic errors and to investigate their effects on cosmological analyses. This work gives JPL the expertise to mitigate key systematic errors affecting the science of the WFIRST[1] and Euclid missions.

Wanted: Fast Simulations

- NASA's Wide-Field Infrared Survey Telescope (WFIRST) and the ESA/NASA Euclid telescope are future space-based missions for studying dark matter and dark energy with key leadership from JPL.
- WFIRST and Euclid will take images of millions of galaxies to probe the underlying dark matter distribution through their positions (galaxy clustering) and shapes (weak lensing).
- An optimal and unbiased cosmological analysis of these data sets requires accurately estimating the errors in the galaxy clustering and weak lensing measurements.
- This can be achieved by producing hundreds or thousands of simulated (or mock) galaxy catalogs. However, traditional simulation methods and complex galaxy formation models require thousands of computing cores for days or weeks to run a single simulation, becoming extremely expensive if this has to be repeated many times.
- This poster presents a simulation code based on approximate methods that is up to 1000 times faster than standard tools, providing an optimal balance between accuracy and speed-up for building hundreds of Euclid and WFIRST simulated surveys.

Methodology

- We run fast dark matter simulations of cosmological structure formation.
- We model galaxy properties using a pragmatic galaxy-halo model, that samples a probabilistic model that connects the different galaxy properties.
- The method takes into account that galaxy properties have evolved over cosmological time.
- Finally, we make the simulated galaxy catalogs more realistic by
- We assess the impact of [illegible] observational systematic in which galaxy measurements are affected b
  the systematics on the observable quantities

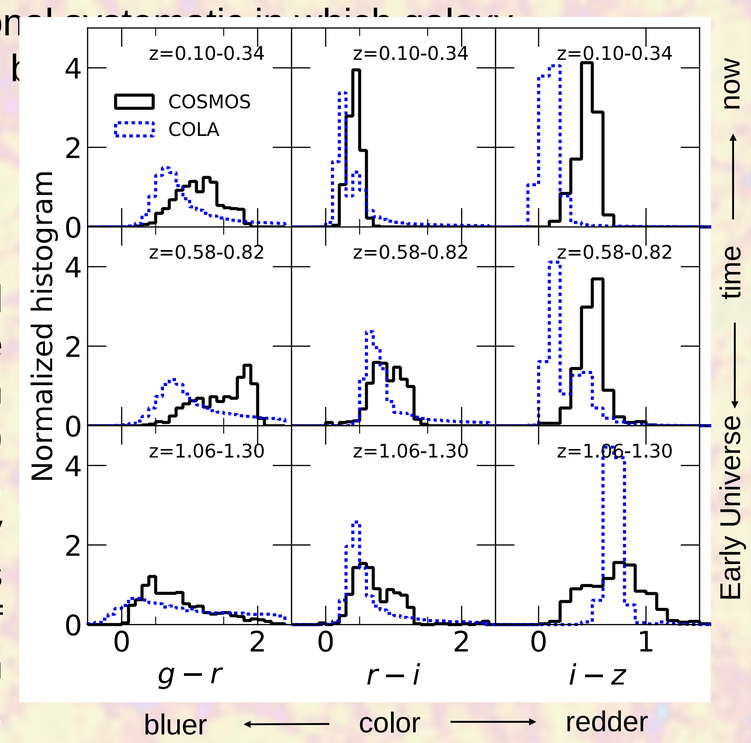

Comparison of simulated galaxy colors (blue) with the Cosmological Evolution Survey (COSMOS) observations (black). Columns and rows display different colors and redshifts respectively. The overlap of the distributions is good for an approximate method.

The power of multi-probe analysis

- Galaxy clustering and weak lensing have different constraining power on cosmological models and are affected by distinct systematics. Combining them provides robust and powerful results.
- Although systematic errors are typically treated as independent between probes, this is not always the case.
- Our fast simulations are unique for predicting in a consistent way both galaxy clustering and weak lensing, therefore letting us model systematics affecting both probes and estimating their impact on Euclid and WFIRST science.

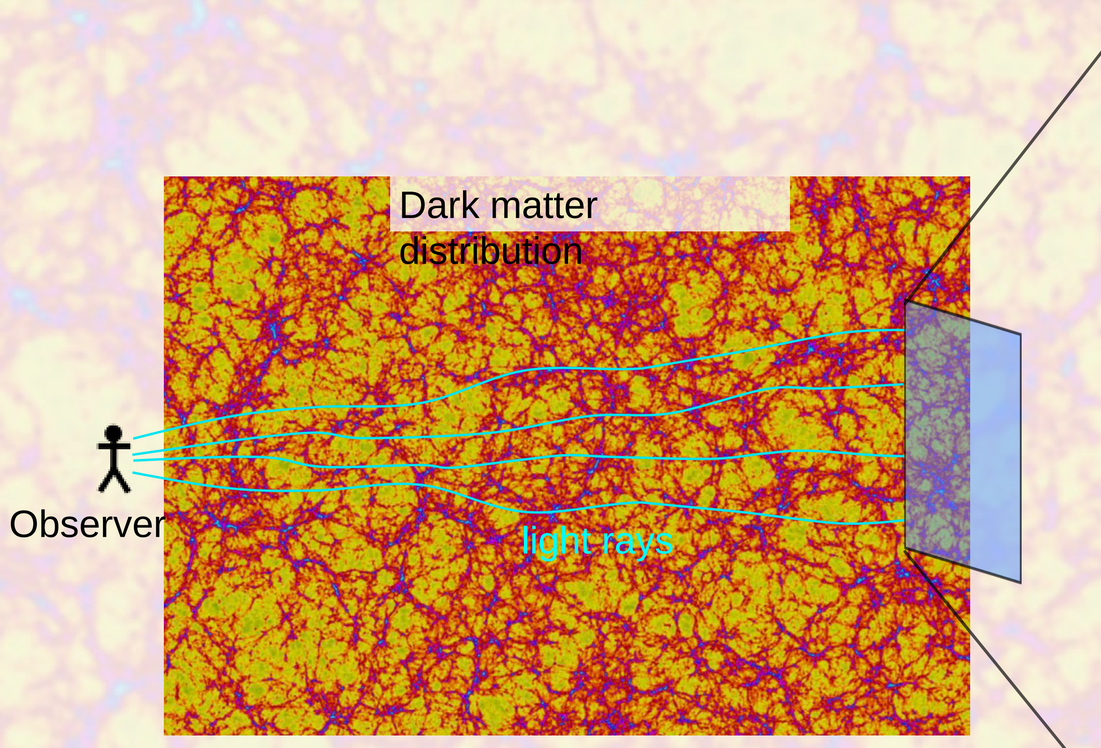

Weak lensing occurs because light-rays coming from distant galaxies are bent by the matter distribution. Our simulations provide consistent predictions for both galaxy clustering and weak lensing.

Future work

- Introduce more systematic effects (such as photometric errors, the selection function) and quantify their impact on science results.
- Construct ~300 survey realizations with the simulations we already have to study the errors on observables.
- Augment the size of the ensemble by running more simulations.

National Aeronautics and Space Administration
Jet Propulsion Laboratory
California Institute of Technology
Pasadena, California

www.nasa.gov

[1]The decision to implement WFIRST will not be finalized until NASA's completion of the National Environmental Policy Act (NEPA) process. This document is being made available for information purposes only.

Poster No. A-06

National Aeronautics and Space Administration

Probing the Structure of the Tr 14 & Carina I Region Using the Stratospheric Terahertz Observatory2

Author: Youngmin Seo[1]

Paul Goldsmith[1], Chris Walker[2], & STO2 Team

[1]Jet Propulsion Laboratory, California Institute of Technology (3266), [2]University of Arizona

I. INTRODUCTION

Life cycle of the interstellar medium & High-mass Star Formation

- [CII] is an important line for investigating the life cycle of ISM but it is not well sampled as it cannot be observed from ground.
- The Carina Nebula is one of the extreme star-forming regions in our Milky Way with a mixture of HII regions, PDRs, CO clumps, and globules.

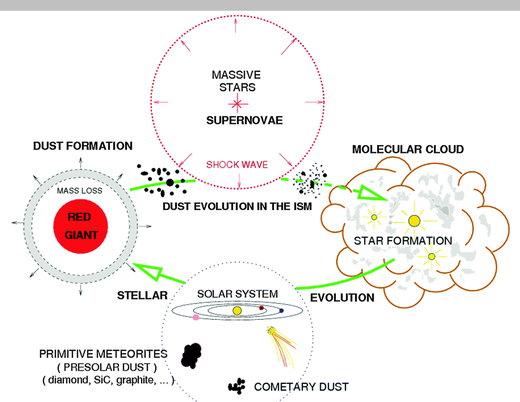

[Bromley et al. 2014]

Goal: Study the ISM structure in a massive star-forming region and understand the interaction of massive stars with their natal clouds in the Carina region.

II. OBSERVATIONS

- Observations using Stratospheric Terahertz Observatory-2
- STO2 is the first high spectral resolution terahertz balloon mission in astronomy
- 0.8-meter telescope, 50″ resolution at 158 μm
- Heterodyne receiver array for [CII]
- Flight from Dec. 9, 2016 to Dec. 28, 2016
- Observed Trumpler14, Eta Carinae, NGC3576, Galactic plane at G310, G328, & G330
- Complementary to Hubble, Herschel, SOFIA, and JWST

III. RESULTS

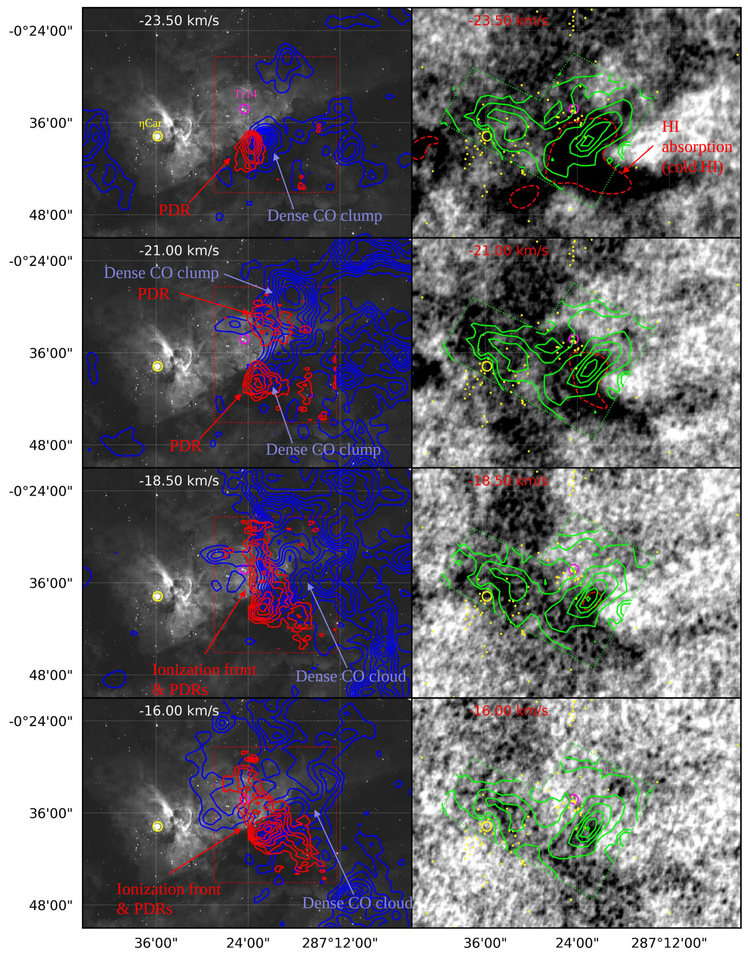

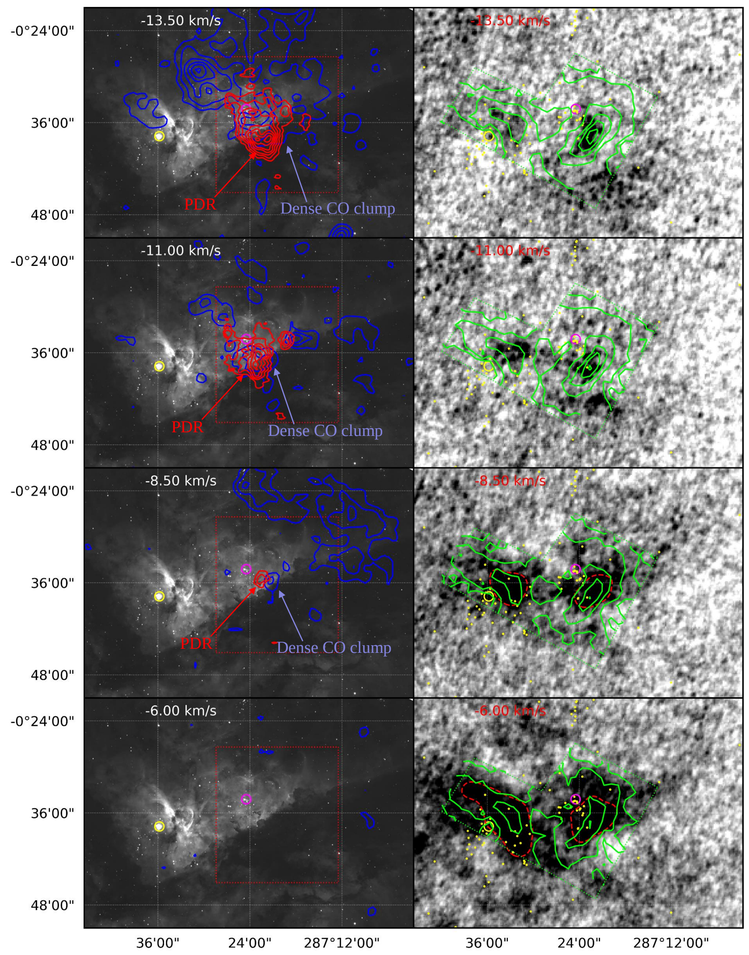

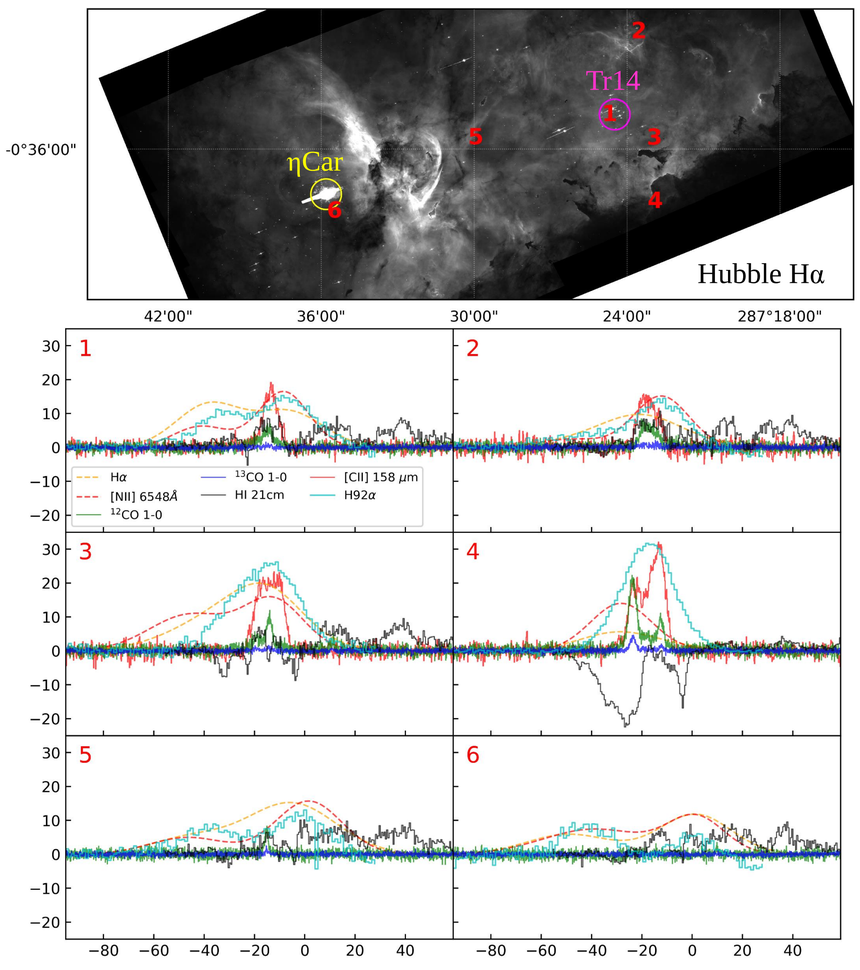

- Left and middle figures: channel maps of [CII] 158 μm, ^{12}CO 1-0 (Rebolledo et al. 2016), H92α (70m DSN; Shinji et al.), and HI 21cm (Rebolledo et al. 2017).
- Left column: contours of [CII] and ^{12}CO overlaid on Hα image. Right column: contours of H92α overlaid on HI 21cm channel maps.
- [CII] contours (red) starting from 1.5 K with steps of 1.5 K, ^{12}CO contours (blue) starting from 7.5 K with steps of 2.5 K.
- H92α contours (green) at 0.25, 0.5, 1, 1.5, 2, 2.5, 3, 3.5, 4 K
- Right figure: spectral lines toward 6 selected positions to probe the ISM structure along the line of sight.
- Coordinates of the image are Galactic coordinates. For spectra, the x-axis is velocity in km/s and the y-axis is antenna temperature in kelvin.

IV. DISCUSSION & CONCLUSION

- STO2 successfully detected [CII] lines and made a large high-resolution spectral map toward Tr14/Carina I
- We found more than 10 dense CO clumps from the Mopra ^{12}CO 1-0 map and their corresponding PDRs in our [CII] map using the high spectral resolution of the data.
- Strong HI absorption features are correlated with dense CO clumps in position-position space (see channel maps). The velocities of the HI absorption features are slightly offset from the velocities of the CO clumps (see spectra on position 4). This indicates that there are expanding cold HI shells on dense CO clumps.
- The double-peaked recombination lines and the velocities of CO clumps suggest that the HII region of Tr 14 is likely an expanding bipolar HII bubble.

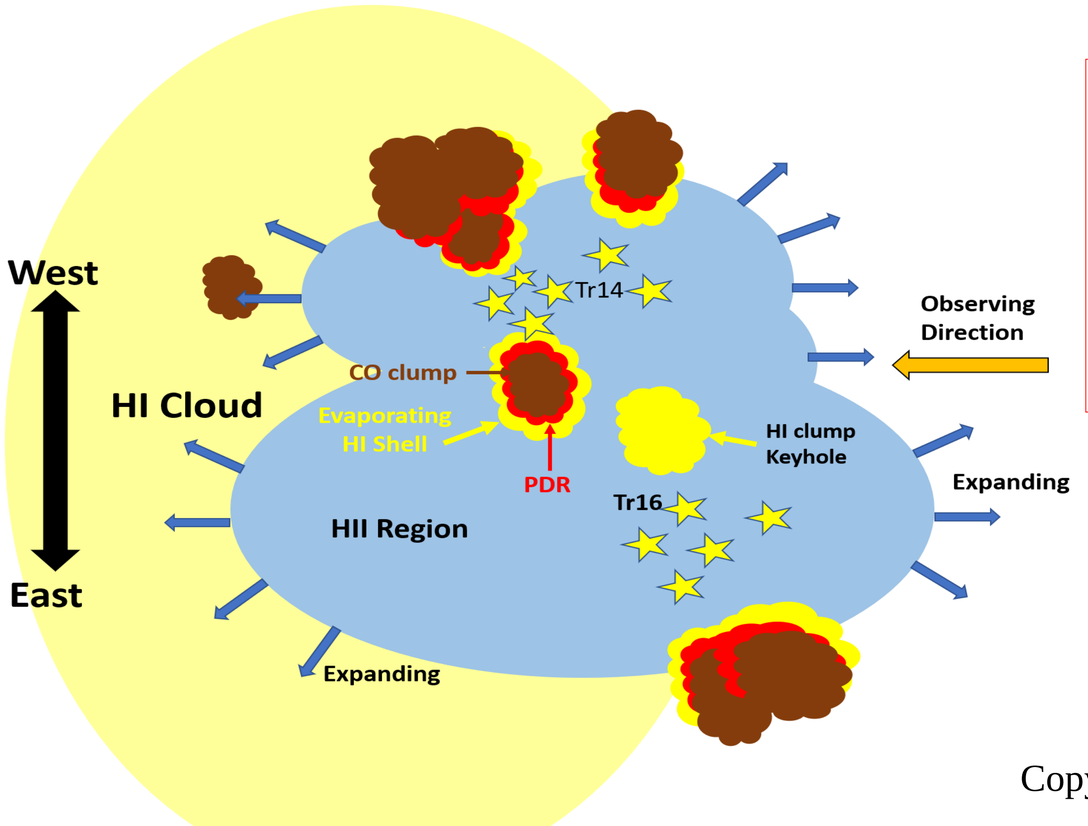

- Based on the kinematics, Tr14/Carina I region has an expanding HII region (Champagne model) and many CO clumps with the corresponding PDRs. (Schematic shown at left)

Poster No. A-07

National Aeronautics and Space Administration

Bias and Uncertainty in Weak Gravitational Lensing Measurements from Photometric Redshifts

Author: Melanie Simet (3266), Rachel Mandelbaum (Carnegie Mellon University)

Background

Weak gravitational lensing is an effect in which the images of distant galaxies are distorted by the gravitational fields the light has passed on its way from the original galaxy to our telescopes.

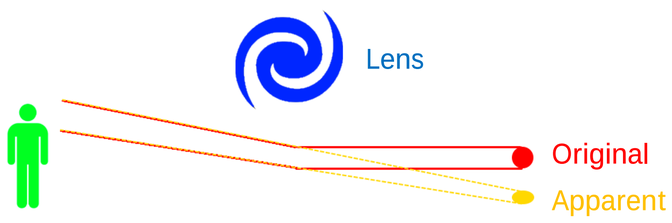

The size of the weak lensing effect depends on the distances to the lens and the distant galaxy. We use **redshift** to determine the distance. For large imaging surveys of the sky, like the one planned for NASA's WFIRST mission, we only have **photometric redshifts**, an estimate of the redshift with uncertainty and potential bias.

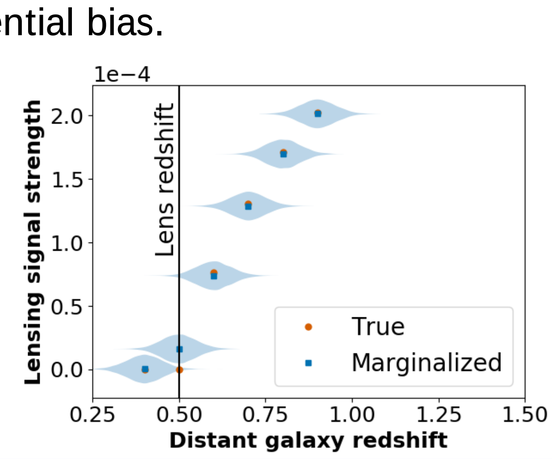

True weak gravitational lensing signal strength compared to the signal marginalized over a Gaussian uncertainty distribution (the filled-in blue curves). Biases appear near the lens redshift.

We must understand the impact of this uncertainty and bias in order to take full advantage of the high-quality data that WFIRST is designed to provide.

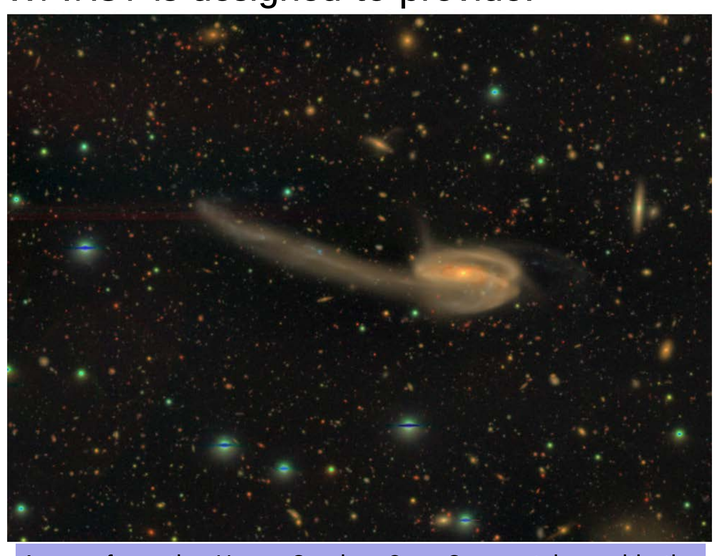

Image from the Hyper Suprime-Cam Survey taken with the Subaru telescope. Weak lensing measurements use the hundreds of small yellow and red galaxies. Image credit: NAOJ

Results

We measure the impact of the uncertainty and bias on lensing measurements due to photometric redshifts by performing numerical simulations. We take real photometric redshift uncertainty distributions from the CFHTLenS data set (Heymans et al 2012) and compare the bias and increased uncertainty from photometric redshift uncertainty. The bias is small, but the uncertainty is increased.

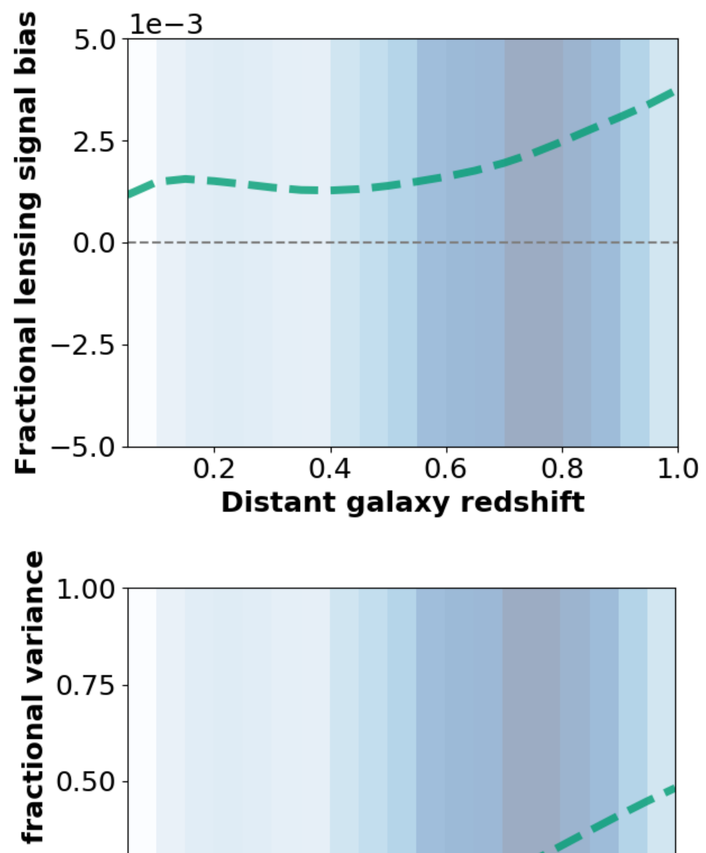

Bias and increased uncertainty due to photometric redshift uncertainty, normalized by the signal strength and the statistical uncertainty, respectively. The distribution of background galaxy redshifts is shown as the blue background color, with darker colors indicating higher density.

This bias is small enough that it will not impact our measurements. And since weak gravitational lensing is intrinsically noisy (with the uncertainty per galaxy being around 100 times the signal), this increased uncertainty is still subdominant.

Our results show that using estimated redshifts will not reduce the quality of weak gravitational lensing measurements with upcoming surveys.

Impact on Future Measurements

- How will better data impact our measurements?

WFIRST's higher data quality will allow us to make better estimates of redshift. Does this improve our weak lensing measurements? We compare the bias and uncertainty from our previous simulation to the values if we reduce the photometric redshift uncertainty in half.

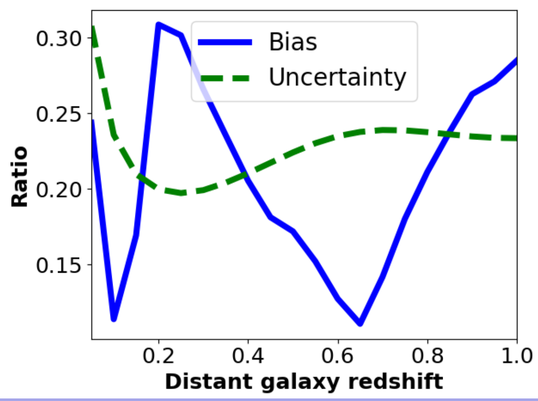

Reduction in bias and uncertainty due to decreased photometric redshift uncertainty. The bias decrease is noisy due to numerical effects from its small amplitude.

We can also investigate what kinds of biases in photometric redshifts matter most. This allows us to set requirements for the performance of upcoming surveys.

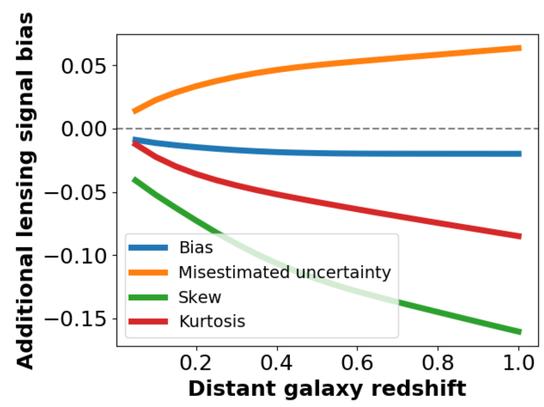

Additional lensing signal bias caused by biases in the photometric redshifts: positional bias, skew, kurtosis, and misestimated uncertainty.

Again, we find that for upcoming surveys, if we have unbiased estimates of the redshift, the quality of our weak gravitational lensing measurements for galaxy-galaxy lensing is not harmed by the use of these estimates.

References

Heymans, C., et al. 2012, MNRAS, 427, 146.

National Aeronautics and Space Administration

Jet Propulsion Laboratory
California Institute of Technology
Pasadena, California

www.nasa.gov

Poster No. A-08

National Aeronautics and Space Administration

Learning about gravity from future cosmological surveys

Jérôme Gleyzes (3268)

Why should why modify gravity?

95% of the Universe is made of unknown components, in particular, 70% is Dark Energy.

While our the picture of Dark Energy as a cosmological constant fits very well the data, it has shortcomings on the theory side, as it does not really work within Quantum Field Theory.

→ Cosmic acceleration could also be caused by modifications of gravity on large scales.

How can we test gravity?

Modifying gravity usually involves adding a new degree of freedom. This is often similar to having some dynamical dark energy (e.g. not a cosmological constant).

→ Many (many) models can do that. We want to test them by their effects on the growth of structure, that is on the distribution of galaxies.

Using an model independent approach.

Along with collaborators we showed that they effects virtually all models can be mapped into five functions of time, within the framework of the Effective Field Theory of Dark Energy (EFT of DE). One can also take the agnostic approach and directly constrain those five functions of time.

Problem: We cannot constrain functions of time, need a small number of (constant) parameters.

Intuition: Not all functions are allowed (they need to obey stability conditions) and that the observables are not sensitive to short scale variations.

To test that, I did the following:

1. Choose five random functions for the EFT of DE, highly complex.
2. Compute the observables.
3. Analyze the observables assuming the EFT of DE can be cast into simple functions
4. Check the goodness of fit

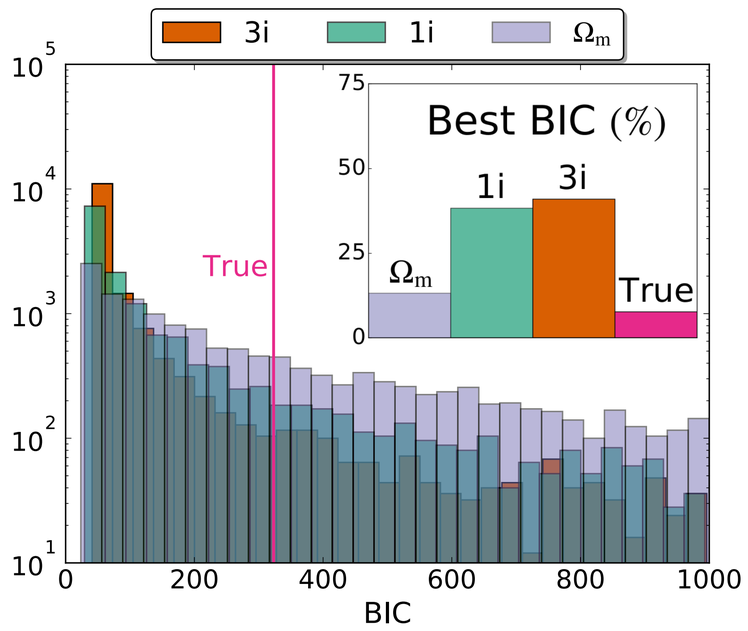

Results:

I compared the BIC (a measure of the goodness of fit which penalizes high number of parameters) using three different basis ('3i', "1i' and Ω_m). 'True' corresponds to the BIC of the original functions (with a high number of parameters). Most of the time, the simple basis with limited number of parameters do better than 'True', functions meaning the initial complexity of the functions is not transferred to the observables. This confirms our intuition, and makes us confident we can use simple basis to perform the analysis of cosmological survey to learn about gravity.

National Aeronautics and Space Administration

Jet Propulsion Laboratory
California Institute of Technology
Pasadena, California
www.nasa.gov

Poster No. A-09

National Aeronautics and Space Administration

Does Planck 2015 Polarization Favor High Redshift Reionization?

Author: Chen Heinrich (326)
Co-author: Wayne Hu (University of Chicago)

How does the CMB probe reionization?

Cosmic microwave background (CMB) E-mode polarization is generated at large scales from scattering of CMB γ with free e^- during reionization, roughly:

Peak height: how much scattering
Peak location: when it happened.

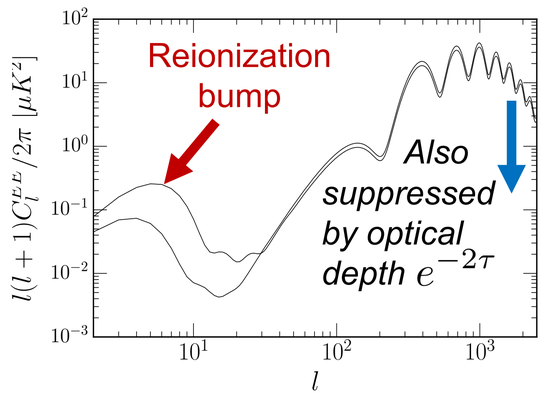

A: **The shape of reionization bump** in low-ℓ C_l^{EE} gives us coarse-grained information on the global ionization history.

How to extract all the information?

A: **Use principal components (PCs)**, the eigenfunctions S_a of Fisher matrix for C_l^{EE} wrt. ionization at different redshifts.

There is more info in the data than traditional tanh can describe

$$x_e(z) = x_e^{\rm fid} + \sum_a m_a S_a(z)$$ (Hu & Holder 03)

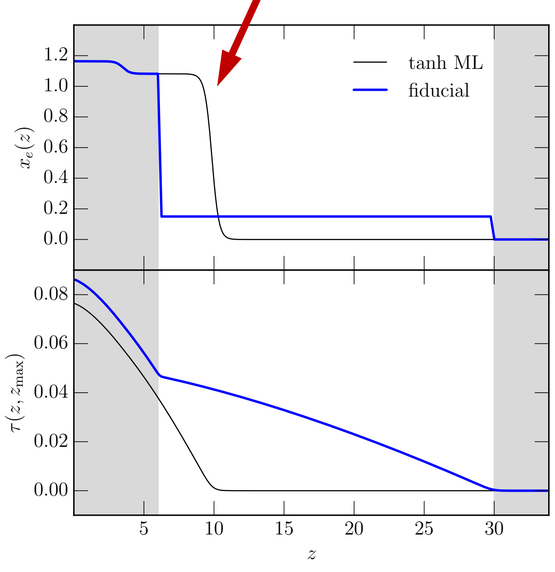

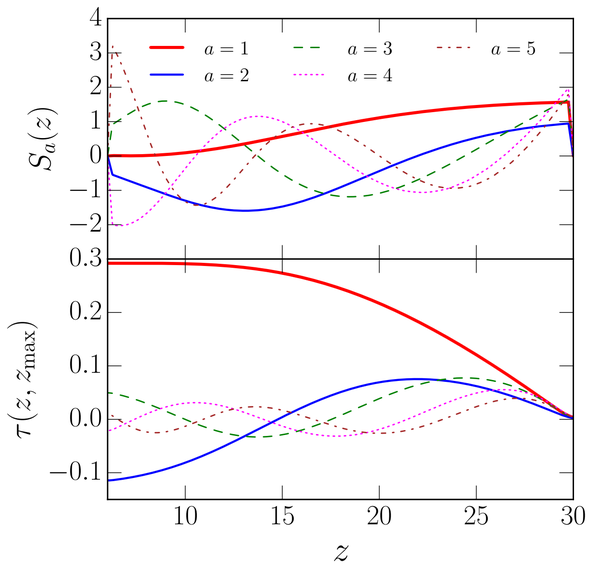

In what sense are PC analyses complete?

A: **PCs reproduce C_l^{EE} of any model to cosmic variance.**

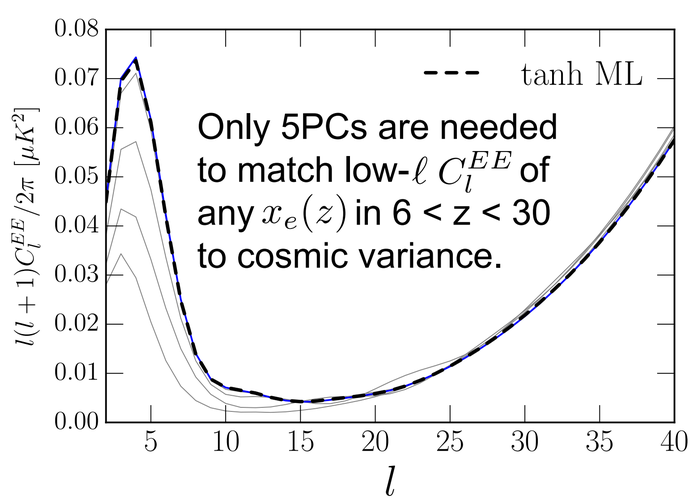

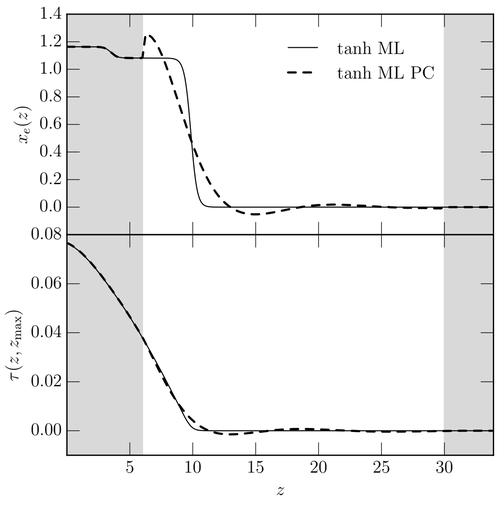

Caution: *PCs not meant to reconstruct $x_e(z)$ (right top), but designed for forward modeling (left). Data better reflected in τ evolution (left bottom).*

Complete Constraints from Planck 2015

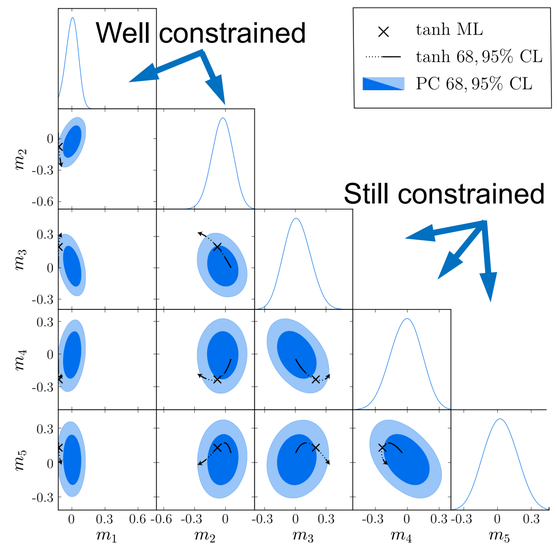

Tanh ML ~2σ away from PC mean

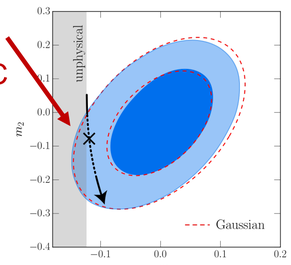

Fast likelihood code:
Now that we extracted all reionization constraints using PCs, we can get the likelihood of any model by projecting $x_e(z)$ unto $\{m_a\}$

Ex.: get tanh results in 5min on a laptop vs. 24 hours MCMC on cluster.

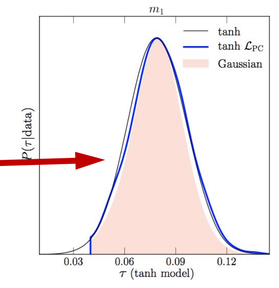

Hint of high-z ionization and origin in the data

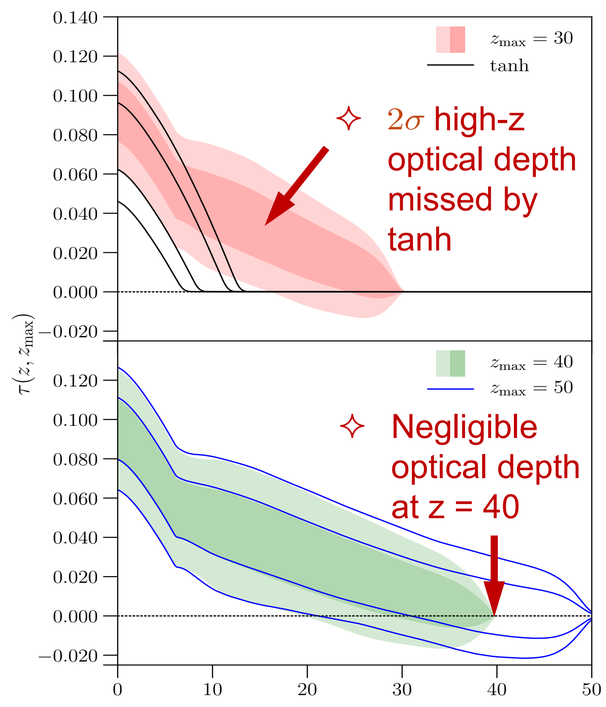

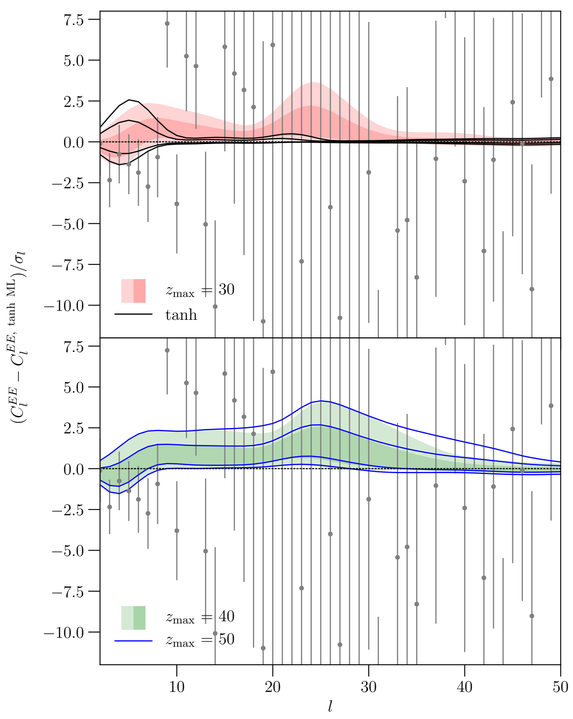

- tanh misses the high-z hint since its functional form assumes negligible ionization before the transition.
- The PC results are stable between zmax = 40 & 50.

Recall: optical depth reflects data sensitivity better than $x_e(z)$

- $l \leq 7$ - Most constraining part.
- $l \sim 10$ - **PCs fit better a few high points than tanh can** as they allow for high-z ionization.
- $l \sim 15 - 20$ - Near cosmic variance limit (CVL)
  $l \gtrsim 30$
  measurements here can better discriminate the high-z regime.

Conclusion

- **For models that allow it, high-z ionization is allowed and even preferred at 2σ level in the Planck 2015 data.**
- For models that don't allow high-z ionization (e.g. tanh), poorer fit indicates **systematic or statistical fluctuations**.
- Origin: higher C_l^{EE} data at $l \sim 10$ than tanh model can fit.
- Planck 2015: weak limit of negligible ionization at z > 40; Next: near CVL C_l^{EE} at $l \sim 15 - 20$ and $l \gtrsim 30$ can do better.

National Aeronautics and Space Administration
Jet Propulsion Laboratory
California Institute of Technology
Pasadena, California
www.nasa.gov

Poster No. A-10

National Aeronautics and Space Administration

A Unified Model of the Emission, Extinction, and Polarization of Interstellar Dust

Brandon S. Hensley (3268) and B. T. Draine (Princeton)

Objective

The goal of this work is the creation of a model of interstellar dust based on non-spherical grains with realistic material properties and sizes which can explain simultaneously and self-consistently all of the observed properties of dust in the diffuse interstellar medium.

What is Dust?

While elements like C, O, Mg, Si, and Fe can exist as atoms or small molecules in interstellar gas, they are often found in macroscopic grains of typical size 0.1μm (10^{-7} m). The grains are thought to come in distinct silicate and carbonaceous varieties.

What Does Dust Do?

Dust grains absorb and scatter light at UV and visible wavelengths, then emit their own radiation in the far-IR. Distant stars and galaxies appear dimmer and redder due to the dust in our Galaxy. Cosmologists studying the Cosmic Microwave Background (CMB) have to carefully separate out the cosmological signal from light emitted by dust in our Galaxy.

Why Model Dust?

The better we understand the physics of dust, the better we can correct for its effects on astronomical observations, enabling higher fidelity science. The nature of dust is also a window into the chemistry and thermodynamics of the interstellar medium. Finally, due to its bright far-IR signal, dust is an excellent tracer of both interstellar gas and the Galactic magnetic field, allowing us to use dust emission to probe the structure of our Galaxy.

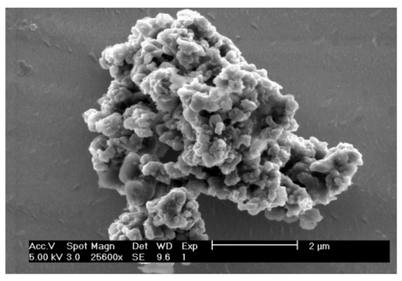

Left: An interplanetary dust particle. We so far have been unable to collect (intact) interstellar grain samples. Image credit: N. Spring.

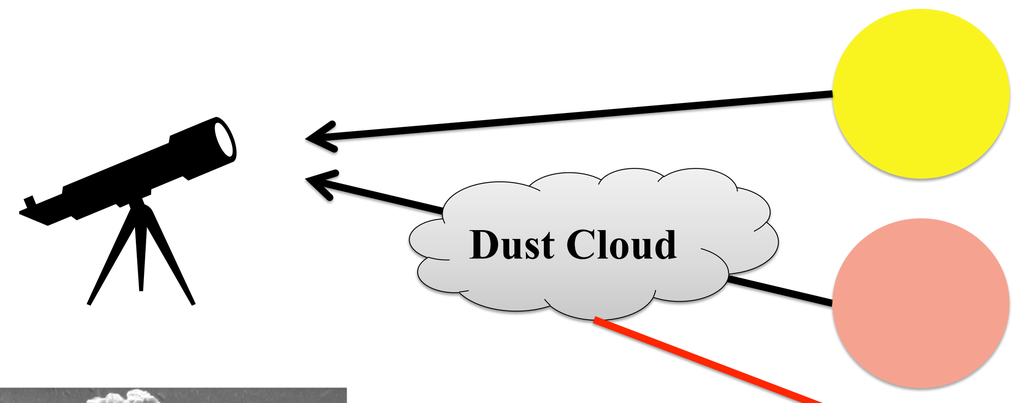

Dust Extinction

Star behind the dust cloud appears redder and fainter than the star with no dust in front of it.

Dust Emission

The dust re-radiates the absorbed starlight at infrared wavelengths.

Journey to a New Model of Interstellar Dust

Dust Modeling Past and Present

We start from the dust model of Draine & Li 2007 which employed carbonaceous and silicate grains to reproduce the observed dust extinction and emission. Draine & Fraisse 2009 extended this model to polarization, but in a consistent way. We build on these work to address these shortcomings of the current generation of dust models:

- Need a self-consistent treatment of polarization, which comes from aligned, aspherical grains.
- Need a self-consistent treatment of the Anomalous Microwave Emission, which comes from spinning ultrasmall grains.
- Need to address known shortcomings in these models, e.g., a factor of ~2 too much extinction per infrared emission, too little mid-infrared extinction, etc.
- Need to update to new observational constraints that have emerged in the last decade, particularly the sensitive far-infrared measurements of dust emission and polarization from the *Planck* satellite

We describe below the series of papers that has resulted from addressing these issues.

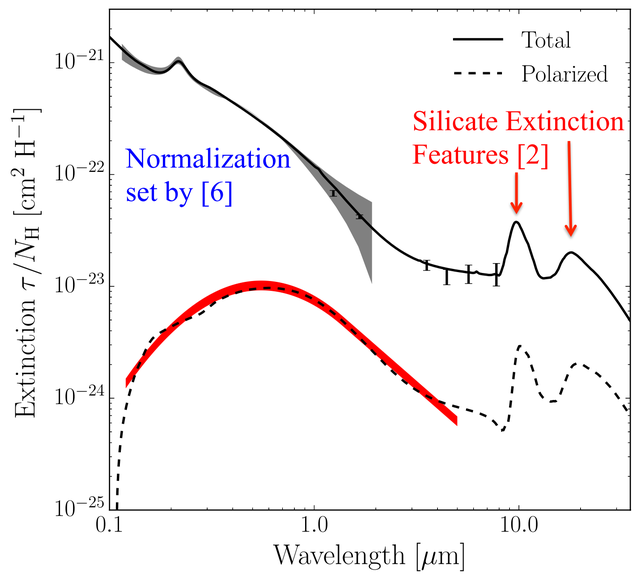

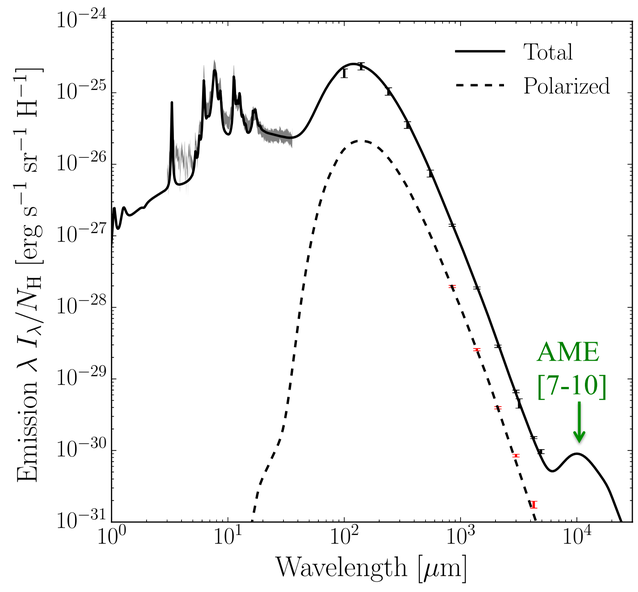

Papers Published While at JPL

We found that Anomalous Microwave Emission (AME) is not strongly correlated with emission from small carbonaceous grains, in conflict with previous models [10]. Thus, we developed new AME models based on small silicate grains [7,8]. A new analysis of quantum effects in ultrasmall grains demonstrated that the grains cannot align with the interstellar magnetic field and thus the AME is expected to be unpolarized [9].

We found that the total dust extinction per hydrogen atom was ~50% lower in the diffuse high latitude sky than the canonical value that has been used since the 1970's [6].

We found that several convenient mathematical functions used to model the distribution of grain shapes led to unphysical results and that certain single grain shapes (e.g., 2:1 oblate spheroids) can approximate integration over more physical shape distributions [4].

Papers Forthcoming

We have reassessed the material properties employed in models of interstellar silicate material on the basis of new spectroscopic observations of the silicate extinction features at 9.7 and 18μm. Using polarization information, we are able to constrain the shapes of interstellar silicate grains, finding them consistent with oblate spheroids [2].

We have compared the polarization properties of dust extinction at UV-visible wavelengths with the polarization properties of dust emission at far-IR wavelengths using a novel "polarization efficiency integral." We find that oblate spheroids with axial ratio 1.4:1 are best at explaining the observed properties [3].

Finally, we have synthesized all of the above into a single, coherent, self-consistent model of interstellar dust, able to explain the observed dust extinction, emission, and polarization with carbonaceous and silicate grains [1]. A comparison to observational data is provided above. While there is room for improvement in future work, this is the most detailed and comprehensive model of interstellar dust do date with wide applications across astronomy.

Benefit to NASA

Interstellar dust affects observations at nearly all wavelengths of astronomical interest. Better dust models enable better correction for the effects of dust, whether in cosmology done with galaxy surveys (e.g., with **WFIRST)** or characterizing stars that host exoplanets. Dust models aid in the interpretation of dust emission, allowing inferences of gas and star-formation properties of galaxies from their infrared emission and identifying the composition and size of particles in protoplanetary disks (both to be studied by **JWST**). Next generation Cosmic Microwave Background experiments searching for the B-mode polarization signature are limited by their ability to model and remove dust emission. Models such as ours can be used to inform the design of future missions and the development of data analysis techniques [5]. Finally, physical dust models probe the chemistry of the interstellar medium and open a new window into the lifecycle of metals.

National Aeronautics and Space Administration

Jet Propulsion Laboratory
California Institute of Technology
Pasadena, California

www.nasa.gov

References

1. Hensley, B. and B. T. Draine. "A Unified Model of the Emission, Extinction, and Polarization of Dust in the Diffuse Interstellar Medium." In prep.
2. Draine, B. T. and B. Hensley. "Interstellar Amorphous Silicates: Grain Shape, Polarization, and Infrared Dielectric Function." In prep.
3. Draine, B. T. and B. Hensley. "Interstellar Amorphous Silicates: Optical and Far-Infrared Polarization." In prep.
4. Draine, B. T. and B. Hensley. "On the Shapes of Interstellar Grains: Modeling Extinction and Polarization by Spheroids and Continuous Distributions of Ellipsoids." Submitted to ApJ. arXiv:1710.08968
5. Hensley, B. and P. Bull. "Mitigating Complex Dust Foregrounds in Future CMB Polarization Experiments." 2018, ApJ, 853, 127
6. Lenz, D., B. Hensley, and O. Doré. "A New, Large-Scale Map of Interstellar Reddening Derived from HI Emission." 2017, ApJ, 846, 38
7. Hensley, B. and B. T. Draine. "Modeling the Anomalous Microwave Emission with Spinning Nanoparticles: No PAHs Required." 2017, ApJ, 836, 2
8. Hensley, B. and B. T. Draine. "Thermodynamics and Charging of Interstellar Iron Nanoparticles." 2017, ApJ, 834, 134
9. Draine, B. T. and B. Hensley. "Quantum Suppression of Alignment in Ultrasmall Grains: Microwave Emission from Spinning Dust will be Negligibly Polarized." 2016, ApJ, 831, 59
10. Hensley, B., B. T. Draine, and A. Meisner. "A Case Against Spinning PAHs as the Source of the Anomalous Microwave Emission." 2016, ApJ, 827, 1

Poster No. A-11

National Aeronautics and Space Administration

Covariances for Cosmology with the WFIRST High Latitude Survey

Elisabeth Krause (326)

Oliver Doré, Tim Eifler, Chen Heinrich, Hironao Miyatake (326)

Motivation:

The most recent history of the Universe experiences a phase of accelerated expansion (see Fig.1), a completely unexpected behavior indicating new and to date undiscovered physics.

Possible Explanations:

- Vacuum energy density (dark energy, cosmological constant)
- Time-dependent scalar field (time-dependent dark energy)
- Modifications to General Relativity (modified gravity)

Cosmology with the WFIRST HLS:

The High Latitude Survey (HLS) of NASA's Wide-Field Infrared Survey Telescope (WFIRST) will provide exquisite measurements the positions and shapes of galaxies over 2000 square degrees to unprecedented depth. From this data set, several cosmological probes can be constructed that are susceptible to cosmic acceleration or modifications to General Relativity in different ways: weak gravitational lensing (cosmic shear), the clustering of galaxies, the abundance of galaxy clusters, and cross-correlations between these probes (galaxy-galaxy lensing, cluster lensing).

The most stringent constraints on cosmic acceleration from WFIRST will be obtained by combing all of these probes in a joint analysis. However, such a joint analysis must account for the correlation between the different probes, i.e. it requires a multi-probe covariance and consistent modeling of correlated systematic effects.

Multi-Probe Analysis Methodology:

We extend the analtic multi-probe covariance formalism presented in Krause & Eifler (2017, MNRAS 470, 2100-2112) to include three-dimensional galaxy clustering measurements (as will be obtained from the WFIRST galaxy redshift survey, GRS) and calculate analytic covariance matrices for cosmological probes customized to the WFIRST HLS specifications. Figure 2 shows a correlation matrix for the cosmological probes from the WFIRST HLS imagaing survey. These covariances consist of

- Gaussian covariance and noise between different two-point statistics
- non-Gaussian covariance, i.e. correlations described by the connected four-point correlation function of the matter density field, which we evaluate using the halo model formalism
- Super-sample covariance, which accounts for the correlation between different modes inside the survey window that are induced by modes on super-survey scales.

These covariances are developed in the CosmoLike framework (www.cosmolike.info), which we also use to implement the multi-probe cosmology analysis with consistent modeling of correlated systematic effects.

Results:

Figure 3 presents forecasts for constraints on the dark energy equation of state from WFIRST HLS. The red, green, and yellow contours illustrate the constraining power of individual probes (galaxy clustering, cosmic shear, galaxy clusters), and the blue contour shows the improved constraints that will be enabled by a multi-probe analysis.

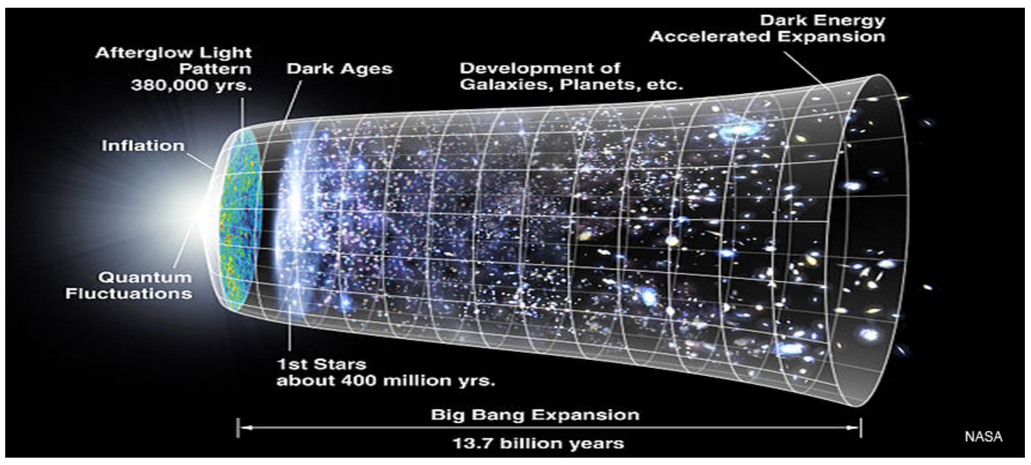

Fig 1: Timeline of the Universe from the early phases of inflation and the Cosmic Microwave Background to today's state of cosmic acceleration.

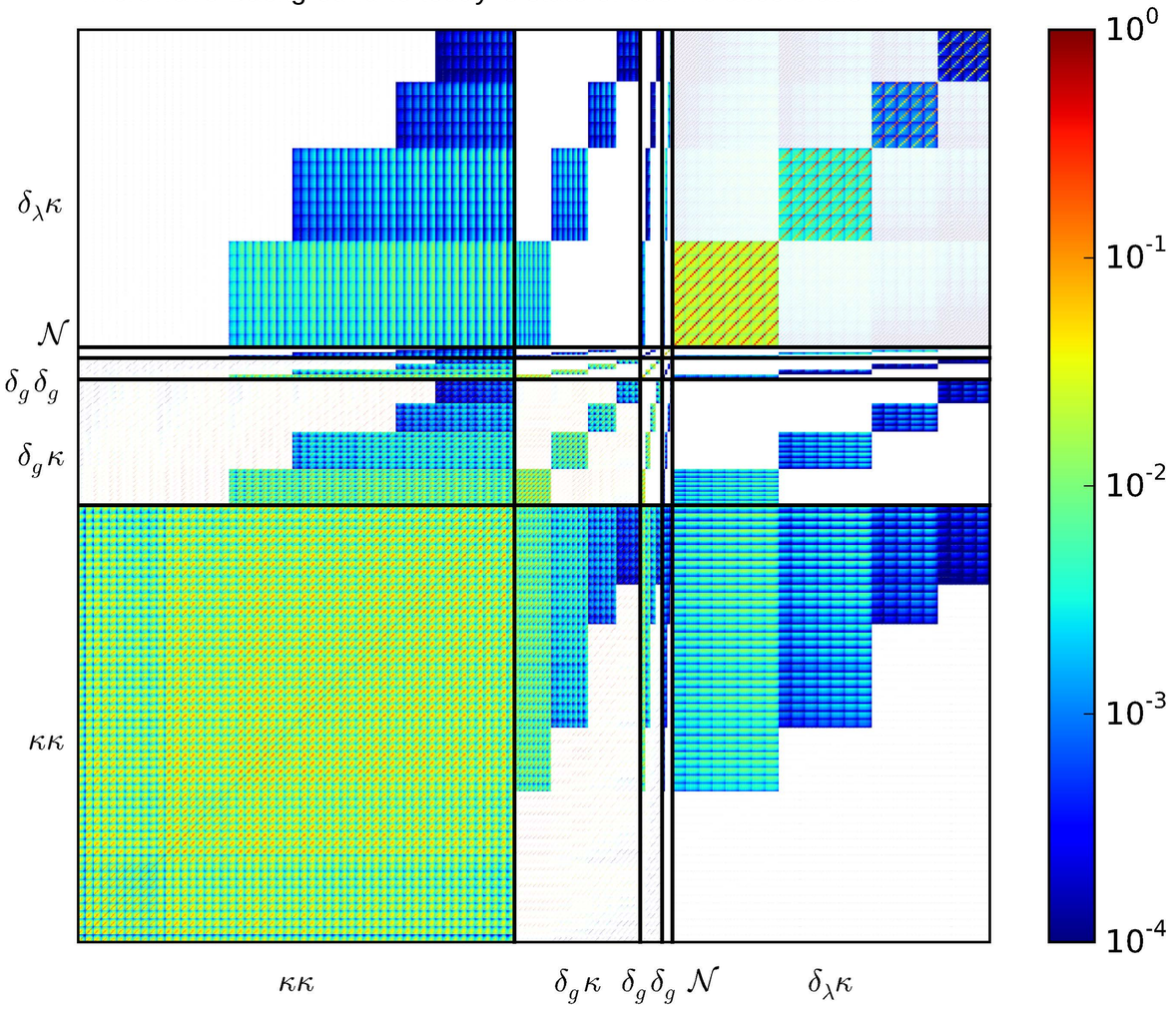

Fig 2: Correlation matrix of cosmological probes that will be measured from the WFIRST HLS imaging survey (left to right: cosmic shear, galaxy-galaxy lensing, galaxy clustering, galaxy clusters number counts, and cluster lensing).

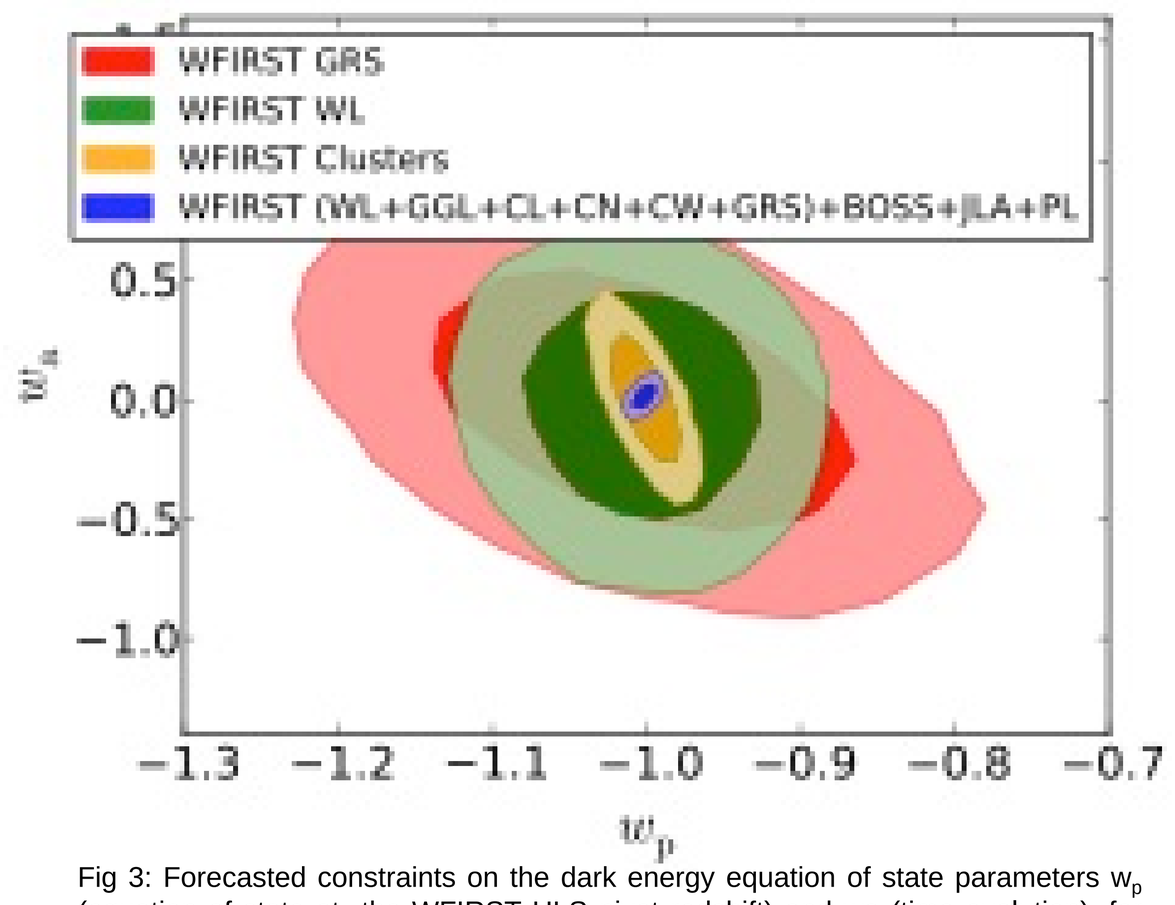

Fig 3: Forecasted constraints on the dark energy equation of state parameters w_p (equation of state at the WFIRST HLS pivot redshift) and wa (time evolution), for individual probes from WFIRST (red, green, yellow contours) and a joint probes analysis (blue contour) of WFIRST probes in combination with priors from current day constraints from supernovae (JLA), baryonic acoustic oscillations (BOSS), and cosmic microwave background (Planck).

National Aeronautics and Space Administration

Jet Propulsion Laboratory
California Institute of Technology
Pasadena, California

www.nasa.gov

The decision to implement the WFIRST mission will not be finalized until NASA's completion of the National Environmental Policy Act (NEPA) process. This document is being made available for information purposes only.

Poster No. A-12

National Aeronautics and Space Administration

New large-scale maps of the cosmic infrared background

Author: Daniel Lenz (3268)
Olivier Doré (3268)

Context

- The cosmic infrared background (CIB) **consists of all the unresolved infrared galaxies** in the Universe
- It is a powerful probe of the astrophysics of galaxies, the star formation history of the Universe, and the **connection between dark and luminous matter**
- The **key challenge** to obtain large-scale CIB maps is the **removal of foreground Galactic dust**

Conclusions

- We have obtained **new, large-scale CIB maps, extracted from the *Planck*** satellite data
- We used **Galactic neutral hydrogen from the HI4PI Survey** to model the Galactic dust foreground
- Our new maps agree well with previous ones, but **cover much larger areas and are subject to fewer systematics**
- The soon-to-be public maps have great legacy value, especially through **cross-correlations and by using them for CMB de-lensing**

Methods: Using HI to model foreground dust

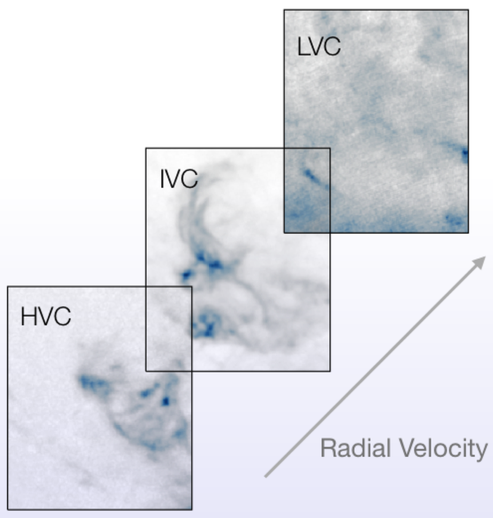

- The **standard approach** to modeling dust emission via HI is manually compute **HI column density maps for different gas phases**
- This requires a **manual separation** of the HI data cube
- Cannot account for complex structures or model large areas

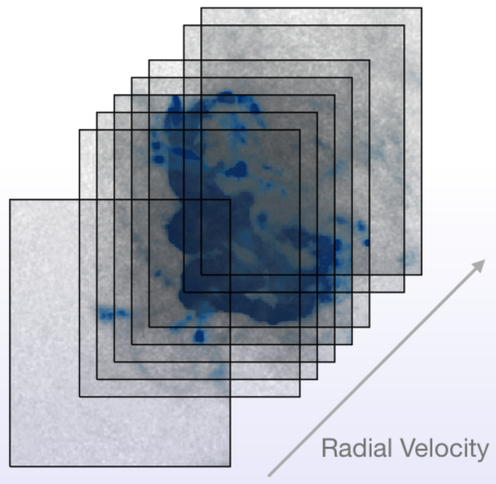

- Instead of accounting only for manually-chosen clouds, we **use each HI spectral channel**
- This allows to **automatically recognize all dust-emitting features**
- The results are **more robust, more accurate** and can be computed **unsupervised**

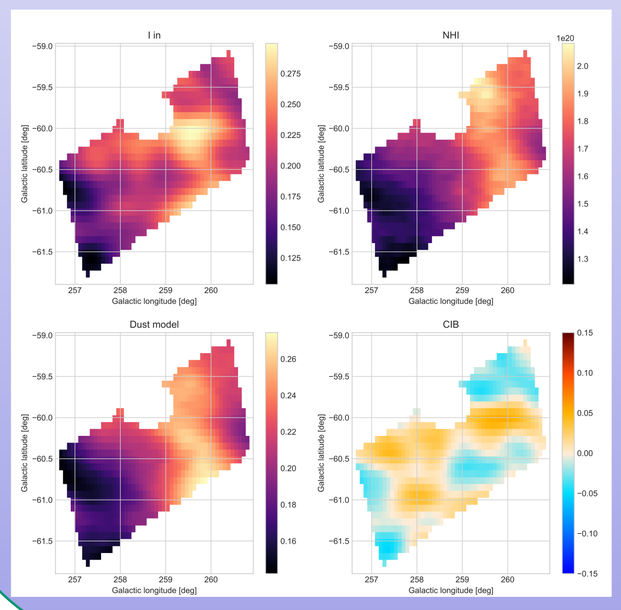

- Spatially, we **perform the component separation on small patches** at a time
- This **reflects variation in the dust-to-gas ratio**
- The main challenge is the ideal choice of spatial scales that **removes most dust, but preserves large-scale CIB fluctuations**

Results: Maps and angular power spectra

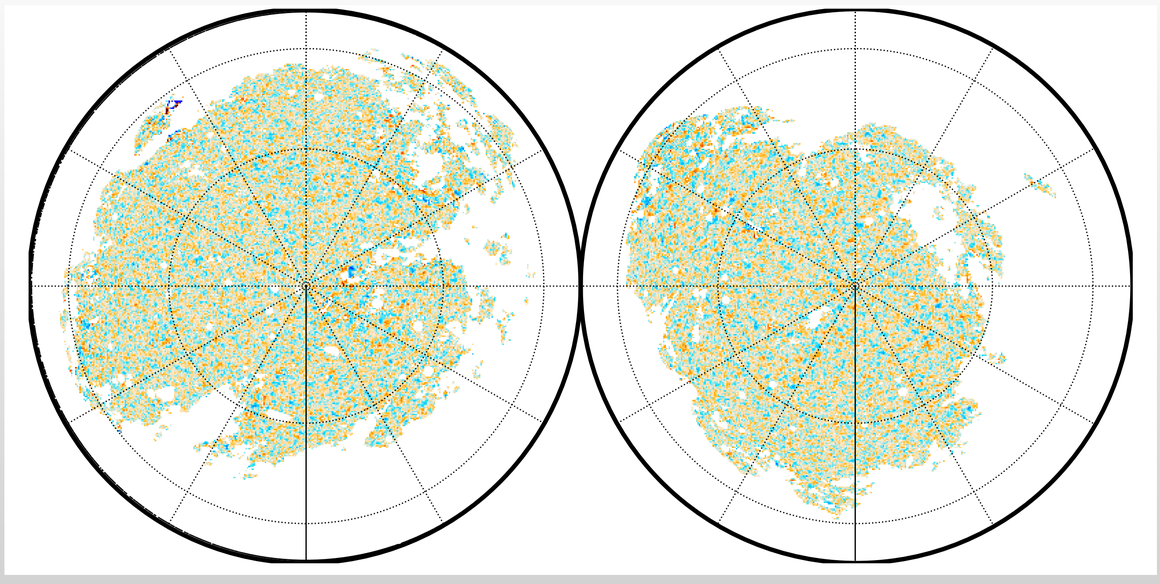

- We obtain CIB maps for **25% of the sky at the highest 5 *Planck* frequencies** (143 - 857GHz)
- On smaller scales, we identify the high quality of the separation through the lack of dust emission for most parts of the sky
- We validate these products **through simulations, internal re-sampling, and comparisons with previous studies**

Cleaned CIB image

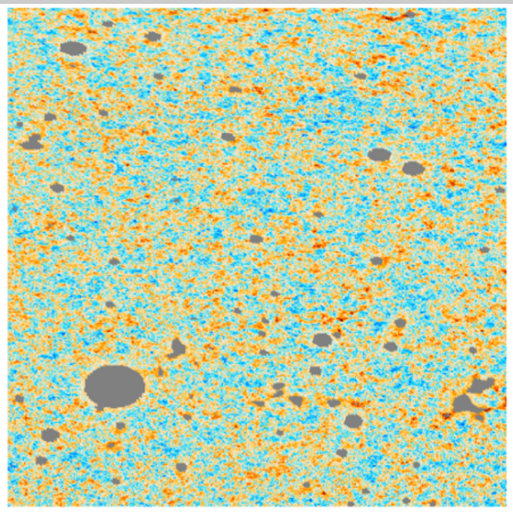

Total FIR intensity

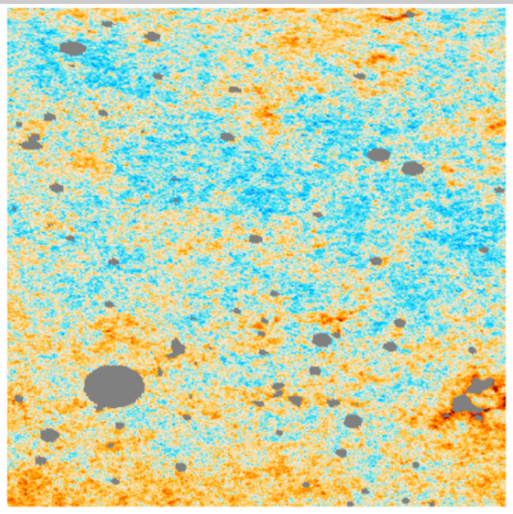

Outlook

- After the initial data release and validation paper, we will present a **detailed modeling of the resulting power spectra**.
- This can be used to **constrain e.g. the primordial non-Gaussianity f_{NL}**
- More sophisticated separation techniques and data sets
  - **Multi-frequency far-infrared data**
  - **Gaia data**
  - **Use galaxy surveys to resolve CIB for smaller areas, create a training sample**

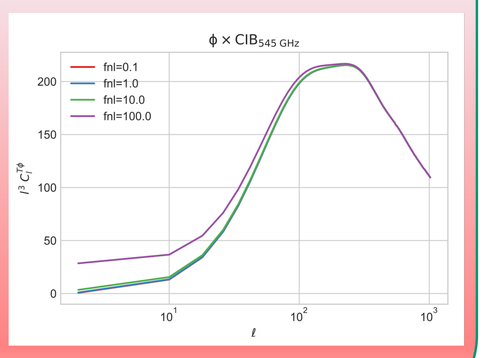

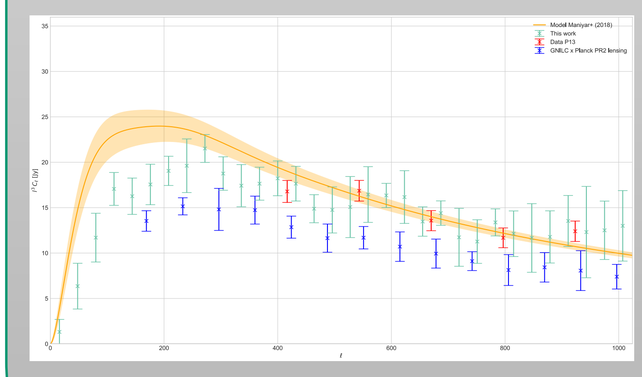

- The **cross-correlation with the *Planck* CMB lensing map** identifies the great overlap in the structures probes through the dusty CIB galaxies and the DM halos
- We obtain measurements on the largest scales, which have **great constraining power for parameters such as the non-Gaussianity f_{NL}**

National Aeronautics and Space Administration

Jet Propulsion Laboratory
California Institute of Technology
Pasadena, California

www.nasa.gov

Poster No. A-13

National Aeronautics and Space Administration

Measuring Galaxy Redshifts for Weak Lensing Cosmology

Daniel Masters (Section 3268)

Collaborators: Daniel Stern (3266), Jason Rhodes (3200), Peter Capak (Caltech/SSC), Judy Cohen (Caltech), Bahram Mobasher (UC Riverside), Dave Sanders (IfA Hawaii)

Context

Understanding the "dark energy" causing the accelerating expansion of the universe is a fundamental goal of the upcoming ESA/NASA Euclid and NASA Wide Field Infrared Space Telescope (WFIRST) missions. A key cosmological probe both missions will use is *weak lensing*, which exploits the fact that the light of background galaxies is deflected by the gravity of intervening matter.

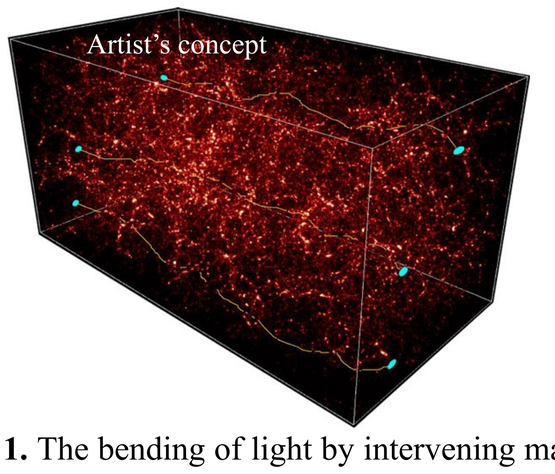

Figure 1. The bending of light by intervening matter as it propagates through the universe. This effect imprints a *correlated shear* in the shapes of galaxies that can be measured statistically in large imaging surveys.

Methodology

We developed a machine learning-based method to map the high-dimensional manifold of galaxy colors that Euclid and WFIRST will measure. The solution we found was the *self-organizing map* or SOM, which projects a high-dimensional data distribution to lower dimensions in a topologically ordered way. We applied this technique to photometry from deep extragalactic fields matched closely in depth and filters to the planned Euclid mission (Masters et al. 2015, 2017).

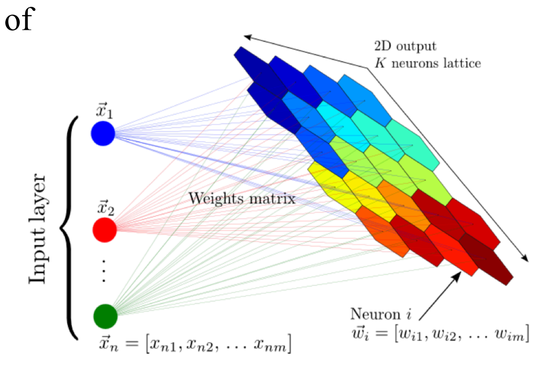

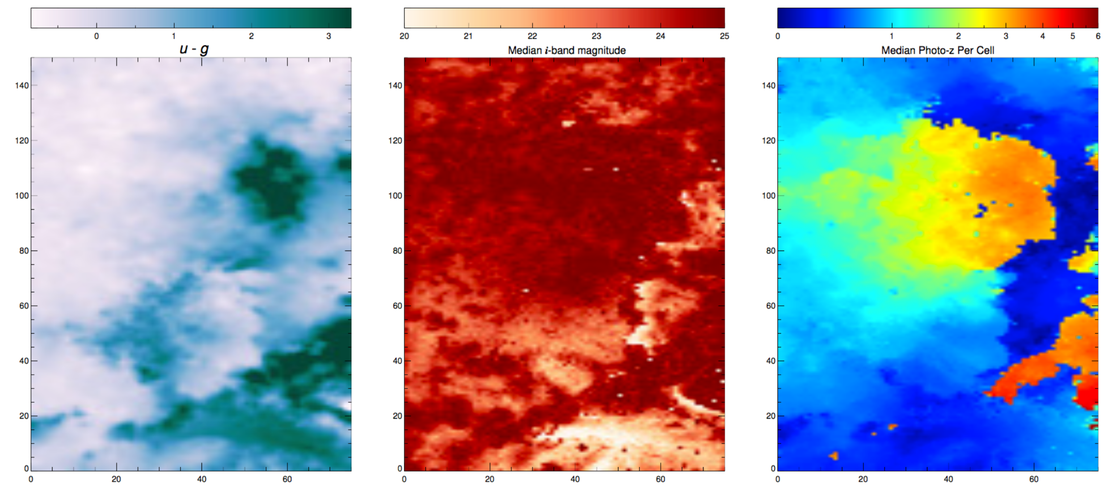

Figure 3. ***Left:*** Illustration of dimensionality reduction with the self-organizing map (from Carrasco Kind and Brunner 2014). ***Right:*** Different views of the SOM we developed from galaxy colors derived using deep field data (Masters et al. 2015, 2017, 2018 (in prep)). Each cell in the SOM represents a galaxy SED that shows up in the data with regularity. This map lets us identify where (in the color space relevant for photo-z estimation) we have sufficient spectroscopic data and where more constraints are needed.

The Redshift Measurement Problem

- To interpret the weak lensing signal, we must know the three-dimensional structure of the galaxies in the lensing sample. Thus we need galaxy *redshifts*, which are related to distance.
- We can only get spectroscopic redshifts for a small fraction of the $>10^9$ faint galaxies that will be imaged by these experiments.
- Therefore we must rely on *photometric redshift* (photo-z) estimates, which use imaging of galaxies in multiple filters to build a low-resolution view of the galaxy spectral energy distribution (SED).
- The requirements on the statistical accuracy of these photo-z estimates are extremely stringent; in particular they must be *highly unbiased.*

The Complete Calibration of the Color-Redshift Relation (C3R2) Survey

- A large, multi-institution, multi-instrument survey with the Keck telescopes to map the galaxy color-redshift relation in preparation for Euclid and WFIRST
- Joint effort of *all* Keck partners (Caltech, NASA, University of California, and University of Hawaii), with JPL leadership
- 44 nights allocated, have obtained ~4500 new spectroscopic redshifts critical to the calibration effort thus far (Masters et al. 2017, Masters et al. 2018 in prep)
- High visibility in community preparing for Stage IV cosmology missions

Principal Investigators:
Judith Cohen (Caltech) – 16 nights (DEIMOS, LRIS, MOSFIRE)
Daniel Stern (JPL) – 10 nights (DEIMOS, NASA Key Strategic Mission Support allocation)
Daniel Masters (JPL) – 10 nights (5 each LRIS/MOSFIRE, NASA Key Strategic Mission Support allocation)
Dave Sanders (IfA) – 6 nights (DEIMOS; upcoming H20 survey will contribute MOSFIRE/LRIS time)
Bahram Mobasher (UC Riverside) – 2.5 nights (DEIMOS)

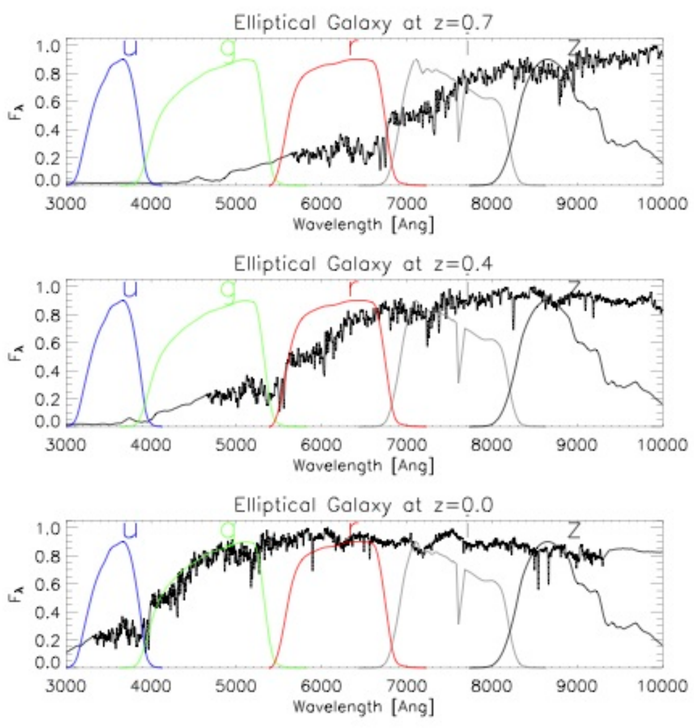

Figure 2. The photo-z estimation principle (from Padmanabhan et al. 2007). As a galaxy's spectrum is redshifted, it will display different fluxes and flux ratios in a given set of broad band imaging filters.

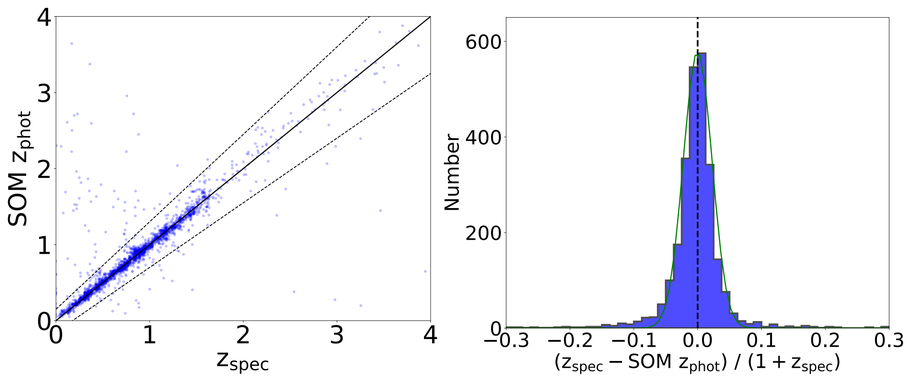

Figure 4. Initial results of the SOM-based calibration applied to the C3R2 spectroscopic sample of ~4500 galaxies obtained in the 2016A-2017A semesters. The method achieves unbiased redshift performance. We are continuing to test and refine the technique with both simulated and real data.

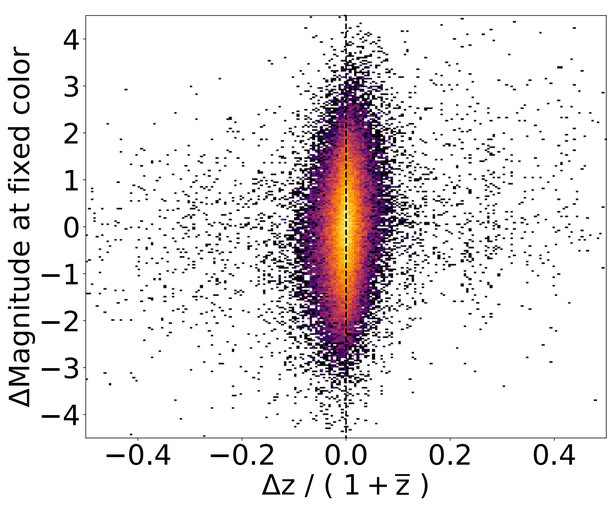

Figure 5. A potentially important result from C3R2: at fixed Euclid/WFIRST color, the brightness of a galaxy carries little additional information about its redshift.

Conclusions

- We have developed a novel method to calibrate galaxy photometric redshifts for cosmology missions.
- Our method forms the basis of the C3R2 survey with the Keck telescopes to prepare for Euclid and WFIRST.

Benefit to JPL

- The C3R2 survey is widely recognized in the cosmology community as *critical* to the success of the Euclid and WFIRST missions, and JPL scientists play a leading role in this effort.
- Powerful machine learning / data visualization technique we developed puts JPL in position make additional major contributions to large-scale galaxy surveys where understanding large, high-dimensional datasets is key.

National Aeronautics and Space Administration
Jet Propulsion Laboratory
California Institute of Technology
Pasadena, California

www.nasa.gov

Poster No. A-14

National Aeronautics and Space Administration

Cluster Weak Lensing with SuperBIT

Authors: Jacqueline McCleary (3268), Eric Huff (3268), Jason Rhodes (3200), Barth Netterfield (U. Toronto), Javier Romualdez (U. Toronto), Steven Benton (U. Toronto), Richard Massey (U. Durham), Sutieng Tam (U. Durham), ***et al.***

Clusters as cosmological probe and why weak lensing rules

•Galaxies like the Milky Way live in gravitationally bound associations called **clusters**
•Clusters form at late cosmological times, when *dark energy* becomes the dominant component of the universe – great probes!
•Clusters are rich in gas and *dark matter* and substructure, and so a great place to study dark matter as well
•Clusters offer a connection to gas/galactic astrophysics due to rich arrays of galaxies they contain

Gravitational Lensing
•Refers to distortion of background object' s light by foreground mass
•In *weak* gravitational lensing (WL), **the signal can only be resolved through averaging large numbers of background galaxies**
•WL is an "**unbiased" mass estimator**, meaning it makes no assumption about the matter doing the lensing!
•WL probes clusters *to the edges of their virial regions*

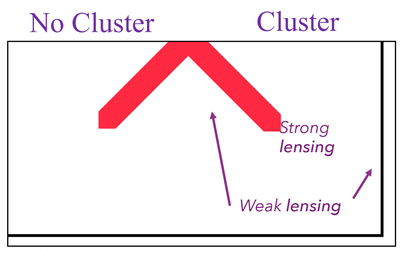

Weak and strong lensing contrasted in images with/without a foreground mass

So what is needed for weak kensing studies? Accurate *shapes*, accurate *distances*, and *large number of sources*

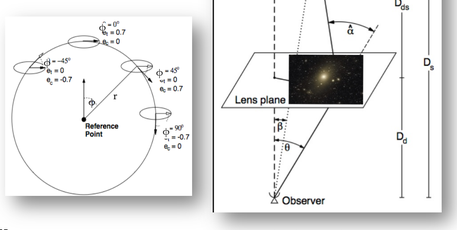

Right: what galaxy "shapes" means here. Left: weak lensing geometry. The clusters we want to measure are on the lens plane!

SuperBIT: an ideal instrument for weak lensing

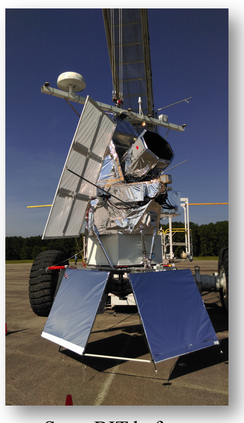
SuperBIT before 2016 test flight

What is SuperBIT?
•SuperBIT = Super-pressure Balloon-borne Imaging Telescope.
•Built with support from NASA-ARPA, Univ. of Toronto and Princeton
•Example of NASA' s *new mid-latitude long duration balloon* capability
•0.5 m mirror, near diffraction-limited PSF, 0.114 square-degree field of view
•Will fly at altitude of 25-35 km

Hubble ACS FOV (11 arcmin^2)

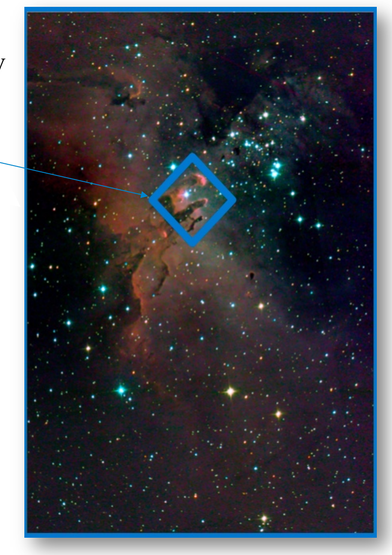
SuperBIT FOV (0.114 deg^2)

Why should cosmologists get excited for SuperBIT?
- 36x the FOV of *Hubble* ACS, with the same resolution!
- Wide field of view gives you many background galaxies behind cluster for **large number of sources**
- **Flies at 25-35 km** so:
  - Predictable, stable observing conditions – space-like!
  - **Diffraction-limited PSF** for **accurate shapes**
  - **Wide wavelength coverage** gives accurate redshifts, which in turn allow **accurate distances**

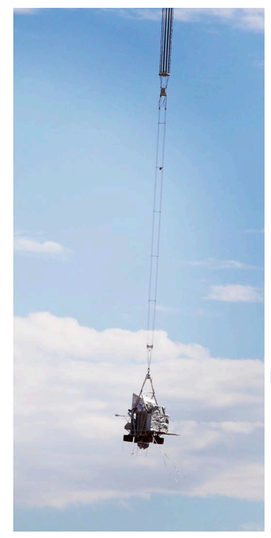
Gondola shortly after launch

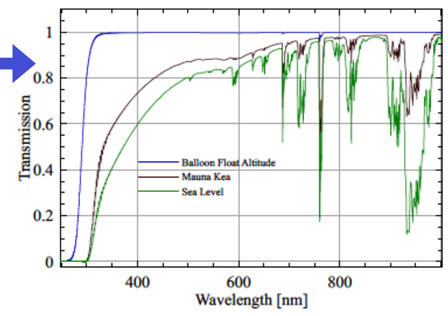

Filter transmission curve for SuperBIT, as compared with terrestrial observatories

Simulations and data reduction pipelines, or the importance of forecasting

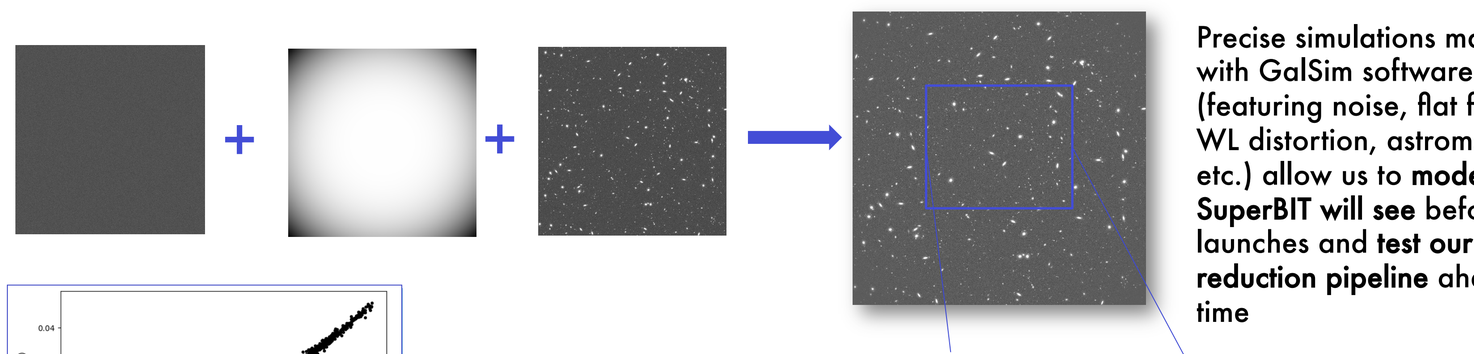

Precise simulations made with GalSim software (featuring noise, flat fields, WL distortion, astrometry, etc.) allow us to **model what SuperBIT will see** before it launches and **test our data reduction pipeline** ahead of time

The data reduction pipeline allows us to compare "real" GalSim shapes to "measured" pipeline shapes, and allows us to **forecast the kinds of clusters SuperBIT can observe most effectively**
- Relaxed Clusters?
- "Bullet" like?
- Work is ongoing!

Things are "looking up"!


View from SuperBIT 2016 test flight

- **Successful test flight** June 2018
- Science flight scheduled for 2019 will image**180 clusters in 5+1 filters**

JPL' s participation in SuperBIT will prepare for other NASA missions. LSST, WFIRST[1], and Euclid are going to revolutionize cosmology, but fast, cheap **SuperBIT-like missions still play a part!**
•SuperBIT UV photometry would break degeneracy in low-z photometric redshifts, which are important for current weak lensing/dark energy studies
•SuperBIT can also help with ground-based surveys' "deblending" woes as they attempt to deconvolve objects that will be clearly distinct to SuperBIT

National Aeronautics and Space Administration
Jet Propulsion Laboratory
California Institute of Technology
Pasadena, California

www.nasa.gov

Poster No. A-15

[1]The decision to implement WFIRST will not be finalized until NASA's completion of the National Environmental Policy Act (NEPA) process. This document is being made available for information purposes only.

National Aeronautics and Space Administration

How Do Star-Forming Galaxies Populate The Cosmic Web?

Author: Alexander I. Merson (3268)

Yun Wang (IPAC, California Institute of Technology), Andrew Benson (Carnegie)

Context

- The majority of the matter in the Universe is thought to be made up of dark matter, distributed in a filamentary-like structure known as the ***cosmic web***. Galaxies are thought to form as gas collapses inside individual dark matter structures called ***halos*** that are embedded in the cosmic web (see Fig. 1). Different types of galaxies are thought to live inside halos of different mass.
- The ESA/NASA Euclid and NASA Wide Field Infrared Survey Telescope (WFIRST) missions will measure the clustering of Hα-emitting galaxies (a type of star-forming galaxy) to probe the nature of dark energy and test for deviations from general relativity.
- **In order to interpret the Euclid and WFIRST clustering measurements we need to know the typical mass of dark matter halos that star-forming galaxies are found in (as a function of the brightness and redshift of the star-forming galaxies).**

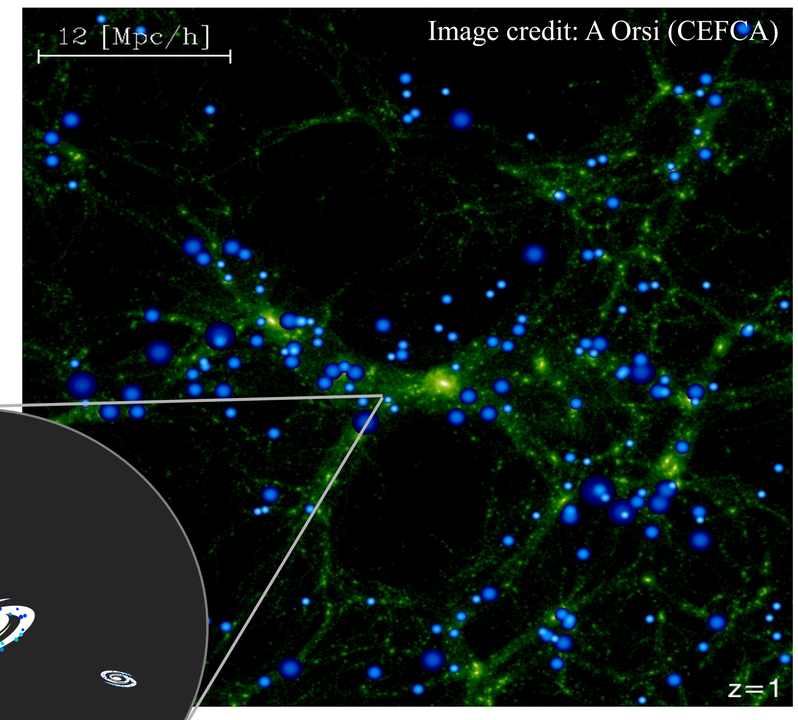

Fig. 1. Simulated star-forming galaxies (blue) embedded in the cosmic web (green). Inset: zoom in of a dark matter halo.

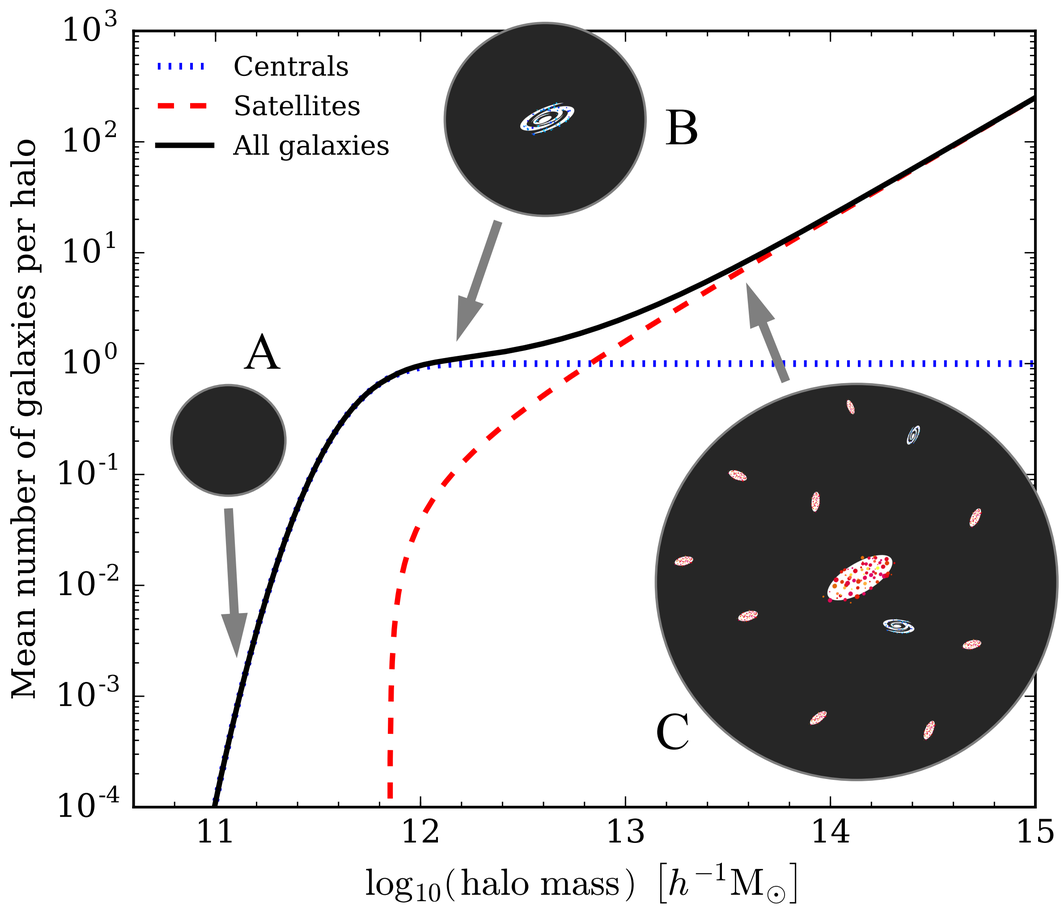

Fig. 2. A schematic of a typical halo occupation distribution (HOD) with images indicating the typical mass scale of an empty halo (A), a halo with a single central galaxy (B) and a cluster of galaxies (C).

The Halo Occupation Distribution (HOD)

- The HOD describes the *mean number of galaxies per dark matter halo as a function of halo mass.* It is often used to help interpret galaxy clustering measurements.
- Very small halos are not massive enough to host any galaxies. As the halo mass increases they become big enough to host a single central galaxy (see Fig. 2).
- The number of central galaxies is typically modeled as a 0-1 step-like function.
- Very massive halos can host clusters of galaxies, with many satellite galaxies, orbiting around a central galaxy. The number of satellite galaxies is typically modeled using a power law above a cut-off halo mass.

Methodology

- We use the galaxy formation modeling software 'Galacticus' (Benson, 2012) to place synthetic galaxies into a population of dark matter halos in a volume of a simulated universe. We work with the dark matter halos from the Millennium Simulation (Springel *et al.* 2005).
- We select samples of the synthetic star-forming galaxies, based upon their brightness, and for each sample compute the halo occupation distribution.

Results

- Our simulation results predict that the HOD for star-forming galaxies is very different to the typically assumed form shown in Fig. 2, particularly for bright galaxies (see Fig. 3).
- Bright star-forming galaxies are found to be central galaxies for 1 in every 10-100 halos with mass 10^{11}–10^{12} $h^{-1}\mathrm{M}_{\odot}$. (1 $\mathrm{M}_{\odot}$= 1 solar mass.)

Benefit to JPL

- With access to state-of-the-art galaxy formation models, such as Galacticus, JPL is able to play a leading role in contributing to our knowledge of galaxy formation theory.
- HOD predictions from galaxy formation models provide a valuable insight for helping interpret clustering measurements that will be made by the Euclid and WFIRST missions.

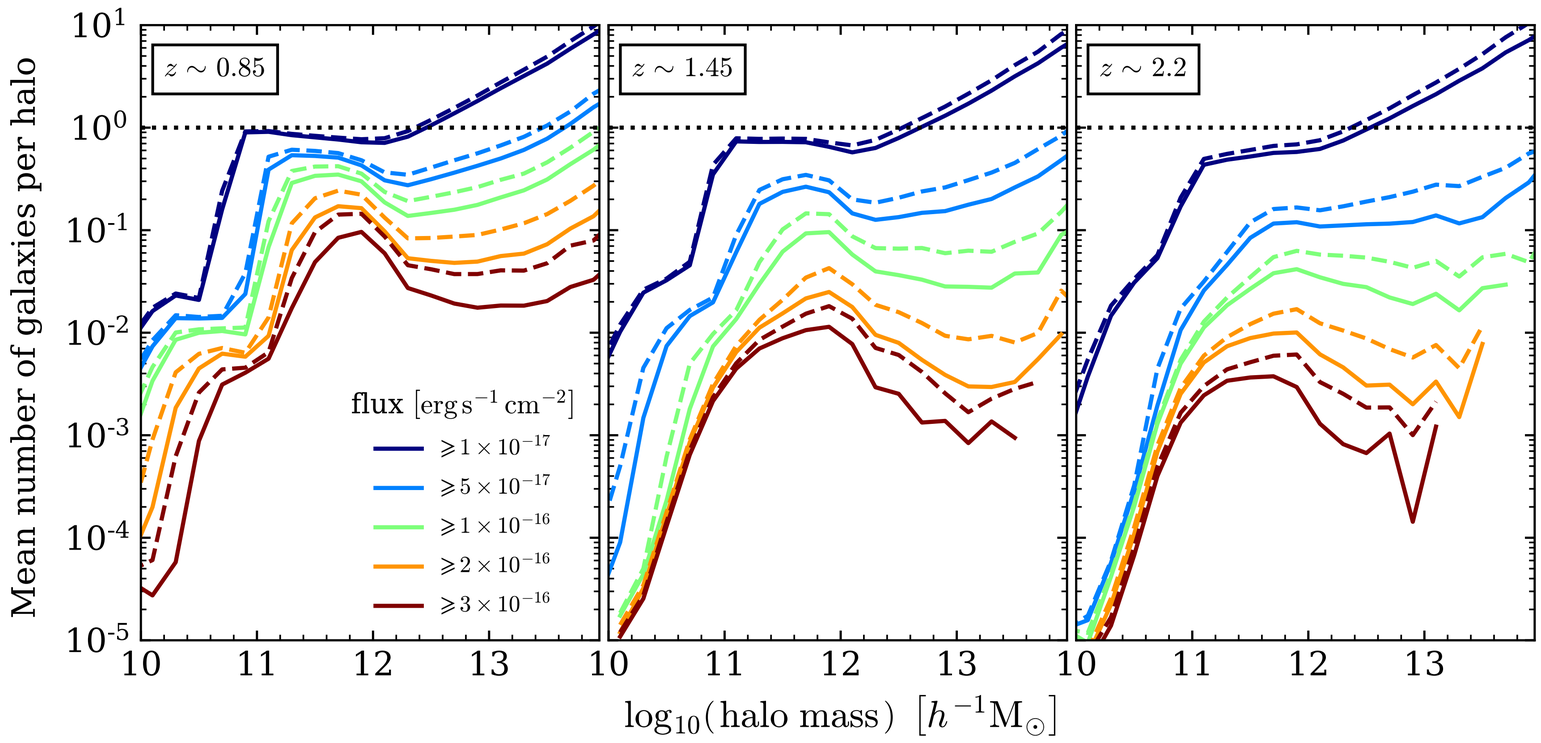

Fig. 3. HODs at three different redshifts (z = 0.85, 1.45 and 2.20) for samples of star-forming galaxies selected according to different brightness (flux) limits, as shown by the different colored lines (ranging from brightest shown in red to faintest shown in blue). Solid lines show the HOD for fluxes attenuated by interstellar dust in the galaxies. Dashed lines show the HODs when dust attenuation is ignored.

National Aeronautics and Space Administration

Jet Propulsion Laboratory
California Institute of Technology
Pasadena, California

www.nasa.gov

Poster No. A-16

National Aeronautics and Space Administration

ROMAN: Reduced-Order Modelling with Artificial Neurons

Alvin J. K. Chua (335S), Chad R. Galley (335S) & Michele Vallisneri (335S)

Overview

ORDER REDUCTION strategies can provide compact representations of modelled waveforms for astrophysical **gravitational-wave** sources, which will facilitate the analysis of data from next-generation detectors such as the **Laser Interferometer Space Antenna** [1].

These representations are obtained by constructing and projecting onto a **reduced-order basis** for the waveform model [2]. However, using them directly in data analysis requires interpolation of the projection coefficients over the model parameter space, which is challenging.

A solution is found within the deep-learning paradigm, where **artificial neural networks** provide a powerful and versatile algorithm for function approximation.

We use deep learning to develop a universal interpolation framework for reduced-order waveform models, and propose several associated **Bayesian inference** techniques for the rapid estimation of source parameters [3].

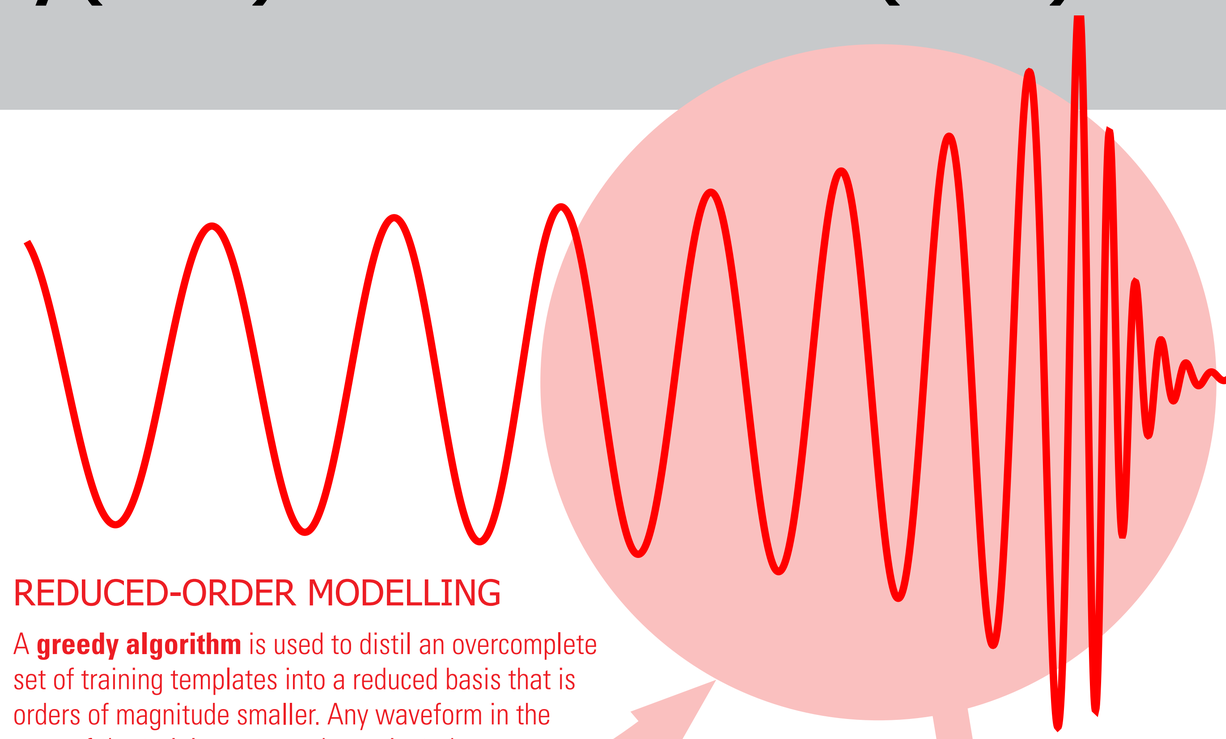

REDUCED-ORDER MODELLING

A **greedy algorithm** is used to distil an overcomplete set of training templates into a reduced basis that is orders of magnitude smaller. Any waveform in the span of the training set may be projected as a linear combination of the basis vectors.

$h(\theta)$ **Waveform template**

Method

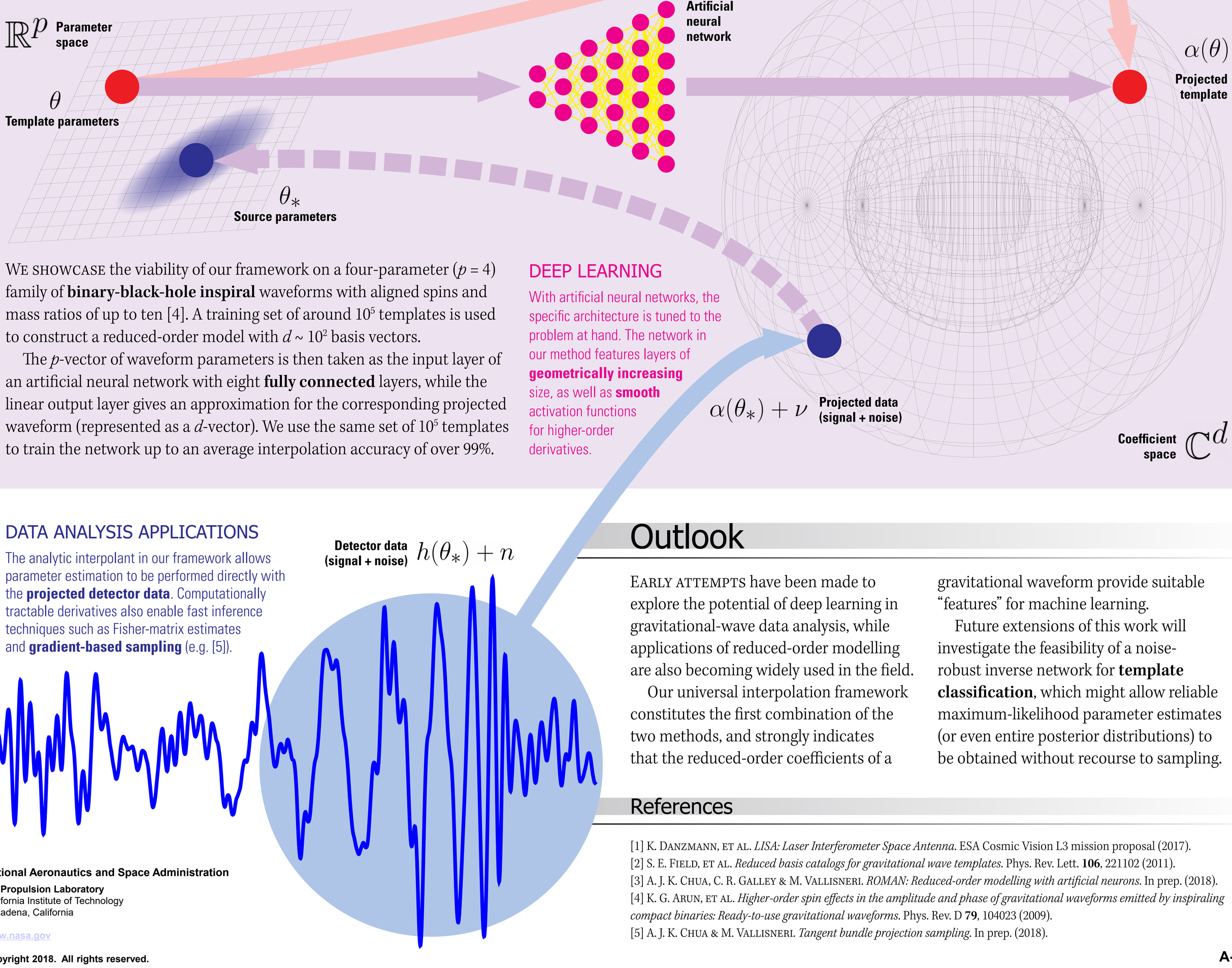

WE SHOWCASE the viability of our framework on a four-parameter ($p = 4$) family of **binary-black-hole inspiral** waveforms with aligned spins and mass ratios of up to ten [4]. A training set of around 10^5 templates is used to construct a reduced-order model with $d \sim 10^2$ basis vectors.

The p-vector of waveform parameters is then taken as the input layer of an artificial neural network with eight **fully connected** layers, while the linear output layer gives an approximation for the corresponding projected waveform (represented as a d-vector). We use the same set of 10^5 templates to train the network up to an average interpolation accuracy of over 99%.

DEEP LEARNING

With artificial neural networks, the specific architecture is tuned to the problem at hand. The network in our method features layers of **geometrically increasing** size, as well as **smooth** activation functions for higher-order derivatives.

DATA ANALYSIS APPLICATIONS

The analytic interpolant in our framework allows parameter estimation to be performed directly with the **projected detector data**. Computationally tractable derivatives also enable fast inference techniques such as Fisher-matrix estimates and **gradient-based sampling** (e.g. [5]).

Outlook

EARLY ATTEMPTS have been made to explore the potential of deep learning in gravitational-wave data analysis, while applications of reduced-order modelling are also becoming widely used in the field.

Our universal interpolation framework constitutes the first combination of the two methods, and strongly indicates that the reduced-order coefficients of a gravitational waveform provide suitable "features" for machine learning.

Future extensions of this work will investigate the feasibility of a noise-robust inverse network for **template classification**, which might allow reliable maximum-likelihood parameter estimates (or even entire posterior distributions) to be obtained without recourse to sampling.

References

[1] K. DANZMANN, ET AL. *LISA: Laser Interferometer Space Antenna*. ESA Cosmic Vision L3 mission proposal (2017).
[2] S. E. FIELD, ET AL. *Reduced basis catalogs for gravitational wave templates*. Phys. Rev. Lett. **106**, 221102 (2011).
[3] A. J. K. CHUA, C. R. GALLEY & M. VALLISNERI. *ROMAN: Reduced-order modelling with artificial neurons*. In prep. (2018).
[4] K. G. ARUN, ET AL. *Higher-order spin effects in the amplitude and phase of gravitational waveforms emitted by inspiraling compact binaries: Ready-to-use gravitational waveforms*. Phys. Rev. D **79**, 104023 (2009).
[5] A. J. K. CHUA & M. VALLISNERI. *Tangent bundle projection sampling*. In prep. (2018).

National Aeronautics and Space Administration
Jet Propulsion Laboratory
California Institute of Technology
Pasadena, California

www.nasa.gov

National Aeronautics and Space Administration

Gravitational Wave Astrophysics with NANOGrav

Author: Joseph Simon (3268)

How does NANOGrav detect Gravitational Waves?

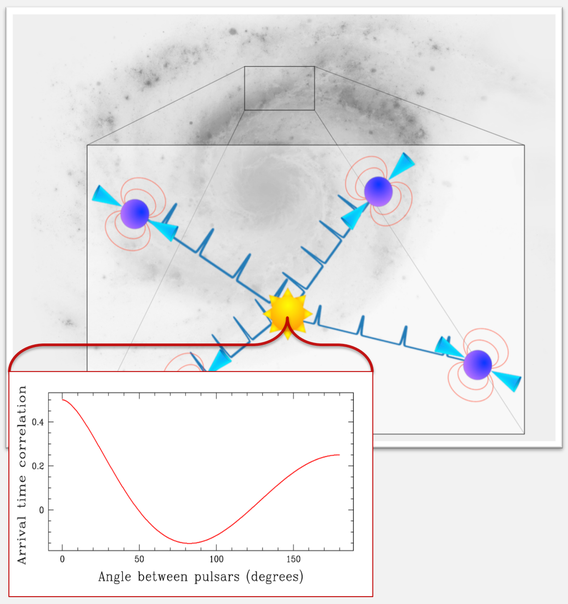

- A galactic-scale nanohertz gravitational wave observatory is created through the monitoring of precisely timed millisecond pulsars, where each pulsar forms an 'arm' similar to those used in LIGO and LISA.
- Millisecond pulsars are a subset of neutron stars: rapidly spinning, detectable as radio sources, timed with atomic clock precision
- Data is correlated from many pulsars, and searched for a distinctive cross-correlation signature [inset], pioneered by Hellings & Downs, caused by a gravitational wave.

Supermassive Black Hole Binaries:
Primary Source of Gravitational Waves for NANOGrav

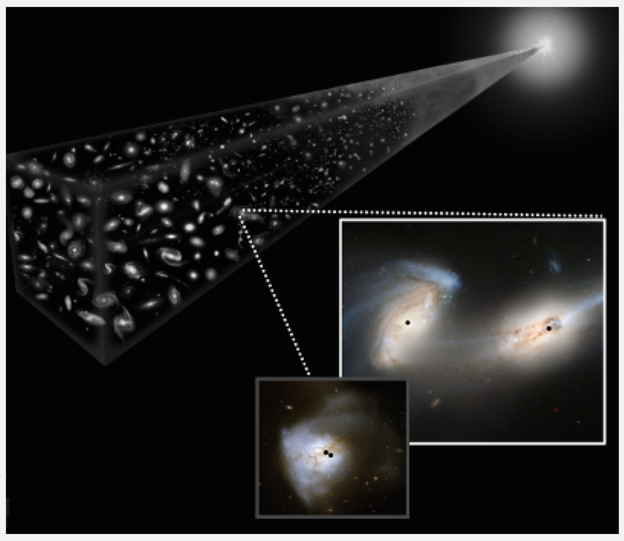

- Hierarchical structure formation predicts that massive galaxies have grown through merging
- Nearby observations reveal supermassive black holes at the center of most massive galaxies with masses correlated to host galaxy properties, implying a shared merger history
- A population of supermassive black hole binaries is produced by the final stages of galaxy mergers

Supermassive Black Hole Binary Evolution

- Dynamical friction drives galaxy mergers, forming a supermassive black hole pair in the newly formed post-merger galaxy core.
- Interactions with gas and stars in the post-merger core dominate a binary's inspiral through parsec separations, hardening the pair and forming tight binary.
- Gravitational radiation provides an efficient inspiral mechanism once the binary reaches sub-parsec separations

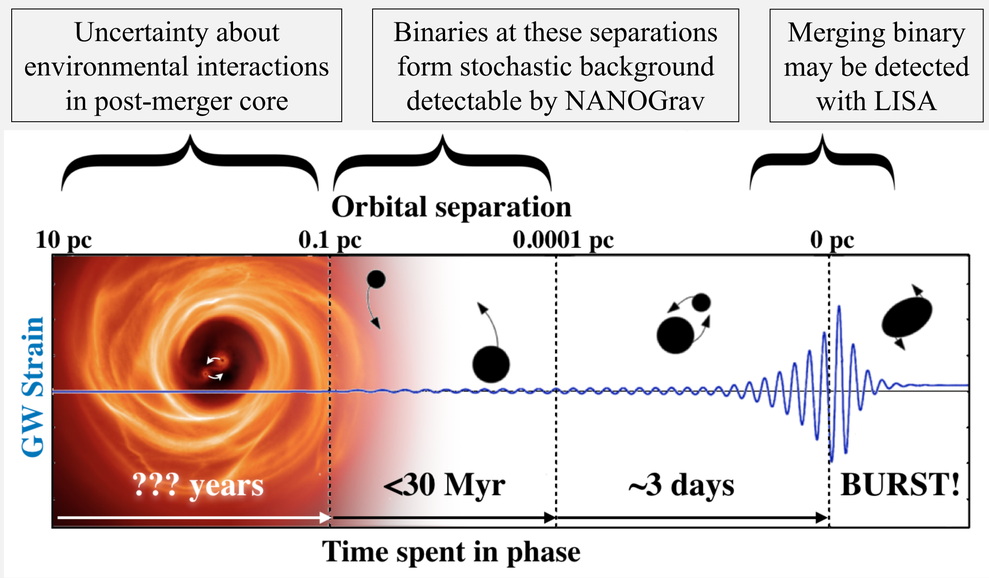

Open Questions

- Binary may stall if interactions with surrounding environment are weak
- Or, strong environmental coupling may quickly drive the binary into the pulsar timing array sensitivity band causing low-frequency attenuation of the stochastic background signal
- Eccentricity may be significantly altered by various interactions with environment

Constraining Binary Evolution Parameters with NANOGrav Data

Simulate Population of Supermassive Black Hole Binaries

Use observed galaxy merger rate and populate galaxies with black holes using black hole mass – host galaxy relation

Model binary evolution under different environments using density of stars, ρ, in the post-merger galaxy core as proxy for environmental strength and the initial eccentricity of the binary orbit, e_0, as it starts to interact with the environment

Simulated Populations with Different Environments

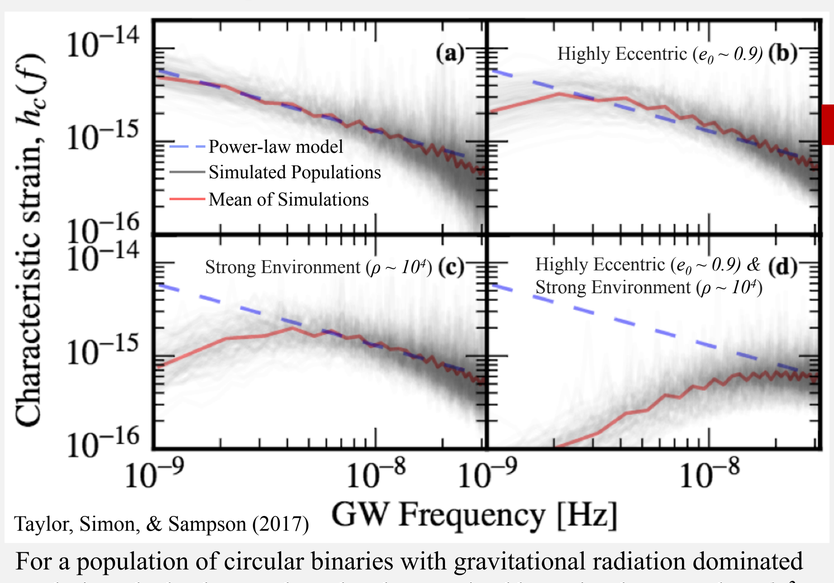

Taylor, Simon, & Sampson (2017)

For a population of circular binaries with gravitational radiation dominated evolution, the background can be characterized by a simple power law, $h_c^2 = A_{yr}^2 (f/\mathrm{yr}^{-1})^{-4/3}$, [blue dashed line], but the mean spectra [red solid line], obtained from one hundred simulated populations [gray shaded region], can vary from that power-law depending on environmental effects.

Gaussian Process Method

Problem: Can't efficiently create a unique set of populations at each point in parameter space

Solution: Train a Gaussian Process on a small set of populations covering entire range of parameter space. Gaussian Process predicts the shape of a gravitational wave background from pulsar timing array data and recovers posteriors directly on model parameters

Direct Posterior on Model Parameters
Creating Environmental Constraints From NANOGrav Data

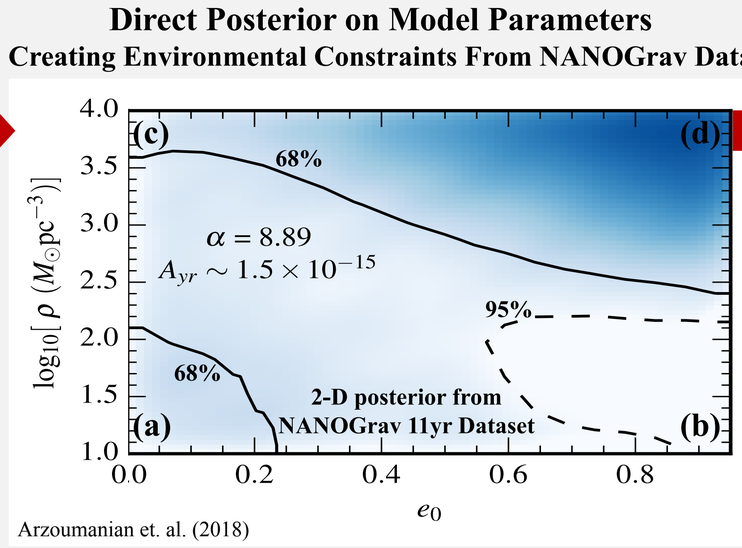

Arzoumanian et. al. (2018)

The four extreme spectra (shown in the plot to the left) map directly to the corners of the recovered posterior, shown above. This mapping is indicated by the corresponding letter in a panel and a corner.
The black hole mass – host galaxy relation is typically expressed as a power law, $\log_{10} M_{BH} = \alpha + \beta \log_{10}(M_{\mathrm{bulge}}/10^{11}\ M_{sun})$. Measurements of this relationship find $\beta \sim 1$, but record varying values for α, based on how they weight individual systems. In the above results, the simulated populations used a relation with $\alpha = 8.89$ and $\beta = 1$, which gives a simple power law background around $A_{yr} \sim 1.5 \times 10^{-15}$.

NANOGrav 11yr Dataset Results

The current, most robust limit on the stochastic gravitational wave background, provided by the 11-year dataset from the NANOGrav collaboration, favors strong environmental couplings and high eccentricities for populations simulated with a large black hole mass – host galaxy relation. This can be seen in the reconstructed spectrum below, which favors a significant low-frequency attenuation. The spectrum is created from the marginalized 2-D posterior recovered by the Gaussian Process method

Spectral Shape from Environmental Constraints

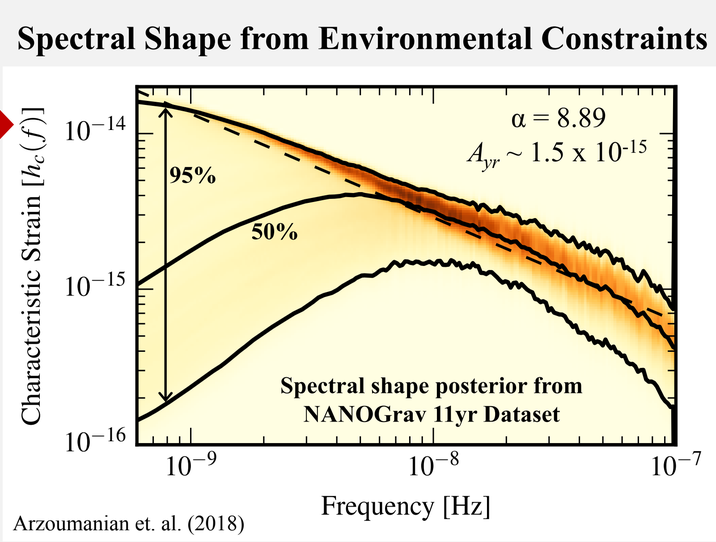

Arzoumanian et. al. (2018)

The 2-D posterior constraints placed directly on the environmental parameters (shown in the blue map to the left) can be mapped into a marginalized spectral shape posterior using the same simulations that trained the Gaussian Process. Above, the marginalized spectral shape posterior is shown. The dashed line indicates the simple power law model prediction. The outer solid lines enclose the 95% region, while the center solid line indicates 50% curve.

National Aeronautics and Space Administration

Jet Propulsion Laboratory
California Institute of Technology
Pasadena, California
www.nasa.gov

Poster No. A-19